European Journal of Chemistry

View Journal Online
View Article Online

Vibrational spectroscopic and Hirshfeld surface analysis of *N*,*N*'-(azanediyl*bis*(2,1-phenylene))*bis*(2-chloropropanamide)

Aysegul Suzan Polat [1,*], Ilkay Gumus [2] and Hakan Arslan [1]

[1] *Department of Chemistry, Faculty of Arts and Science, Mersin University, Mersin, 33343, Turkey*
aysegul.polat@mersin.edu.tr (A.S.P.), hakan.arslan@mersin.edu.tr (H.A.)
[2] *Department of Basic Sciences, Faculty of Maritime, Mersin University, Mersin, 33343, Turkey*
ilkay.gumus@mersin.edu.tr (I.G.)

* *Corresponding author at: Department of Chemistry, Faculty of Arts and Science, Mersin University, Mersin, 33343, Turkey.*
Tel: +90.533.5671703 Fax: +90.324.3610047 e-mail: aysegul.polat@mersin.edu.tr (A.S. Polat).

RESEARCH ARTICLE

10.5155/eurjchem.10.4.386-402.1921

Received: 02 September 2019
Received in revised form: 22 October 2019
Accepted: 26 October 2019
Published online: 31 December 2019
Printed: 31 December 2019

KEYWORDS

Vibration spectrum
Ab initio calculations
Infrared spectroscopy
Redox active compound
Density functional theory
Hirshfeld surface analysis

ABSTRACT

The title molecule, *N,N'*-(azanediyl*bis*(2,1-phenylene))*bis*(2-chloropropanamide) (L^{NNN}) was synthesized and characterized by means of Hirshfeld surface analysis and vibrational (FT-IR and RAMAN) studies. Ab-initio Hartree-Fock (HF) and density functional theory (DFT; BLYP, B3LYP, B3PW91 and mPW1PW91) calculations were accomplished using 6-31G(d,p) and 6-311G(d,p) basis sets. The comparison of calculated bond lengths and angles with X-ray crystal structure shows sufficient agreement. The solid phase FT-IR and FT-RAMAN spectra of L^{NNN} have been recorded in the regions 4000-525 cm^{-1} and 4000-50 cm^{-1}, respectively. A comparative analysis between the calculated and experimental vibrational frequencies was carried out and significant bands were assigned. The results indicated a good correlation between experimental and theoretical IR and RAMAN frequencies. A detailed analysis of the intermolecular interactions *via* Hirshfeld surface analysis and fingerprint plots revealed that supramolecular structure of the L^{NNN} is stabilized mainly by the formation of H···H, C···H, Cl···H ve O···H intermolecular interactions.

Cite this: *Eur. J. Chem.* **2019**, *10(4)*, 386-402 **Journal website**: www.eurjchem.com

1. Introduction

Recently, many of research groups focused on the development of highly efficient and selective catalysts [1-7]. The catalytic activity performance of metal complexes depends on the interaction of the metal center and its surrounding ligands. Redox non-innocent or redox active ligands, unlike classical ligands, are actively involved in redox processes [8-22]. So, they supply an opportunity to modify the reactivity of metal complexes. As an example, Smith *et al.* found that the metal-carbon bond formation for Negishi-like cross-coupling of alkyl halides with organozinc reagents can occur via metal-centered oxidative addition steps but without changing the *d*-electron configuration of the metal [23]. The required electrons were supplied by redox active ligands and so, redox active ligands offered selectivity to the metal complex for the catalytic activity.

Considering the facts above, the intent of this study is to perform an experimental and computational work on a potential redox active compound, *N,N'*-(azanediyl*bis*(2,1-phenylene))*bis*(2-chloropropanamide) (L^{NNN}). The optimized geometric parameters and vibrational frequencies have been calculated using the HF method with 6-31G(d,p) and 6-311G(d,p) basis sets and similarly with DFT (BLYP, B3LYP, B3PW91 and mPW1PW91) methods along with 6-31G(d,p) and 6-311G(d,p) basis sets. In addition, intermolecular interactions and packing modes present in the solid state of the title compound were visualized by means of the Hirshfeld surface analysis.

2. Experimental

2.1. Instrumentation

The NMR spectra were recorded in $CDCl_3$ solvent on Bruker Avance III 400 MHz NaNoBay FT-NMR spectrophotometer using tetramethylsilane as an internal standard. FT-IR and FT-RAMAN spectroscopy was used for the identification of vibrational modes in the L^{NNN} molecule. The room-temperature-attenuated total reflection Fourier transform infrared (FT-IR ATR) spectrum of *N,N'*-(azanediyl*bis*(2,1-phenylene))*bis*(2-chloropropanamide) compound was recorded using a Perkin Elmer Spectrum 100 series spectrometer with a ATR prism (4000-525 cm^{-1}; number of scans: 250; resolution: 1 cm^{-1}) (Figure 1).

ISSN 2153-2249 (Print) / ISSN 2153-2257 (Online)
http://dx.doi.org/10.5155/eurjchem.10.4.386-402.1921

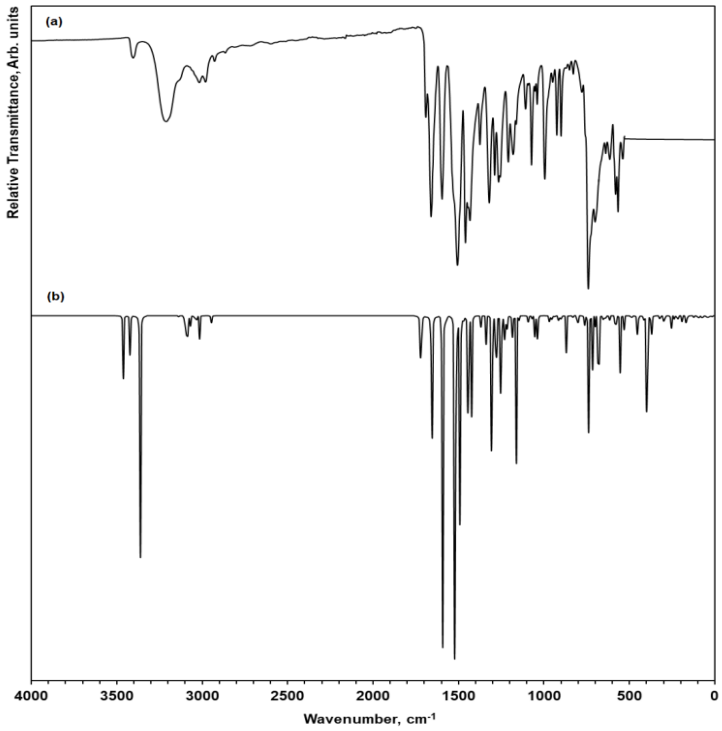

Figure 1. Experimental (a) and theoretical (b) FT-IR spectrum of L^{NNN} compound.

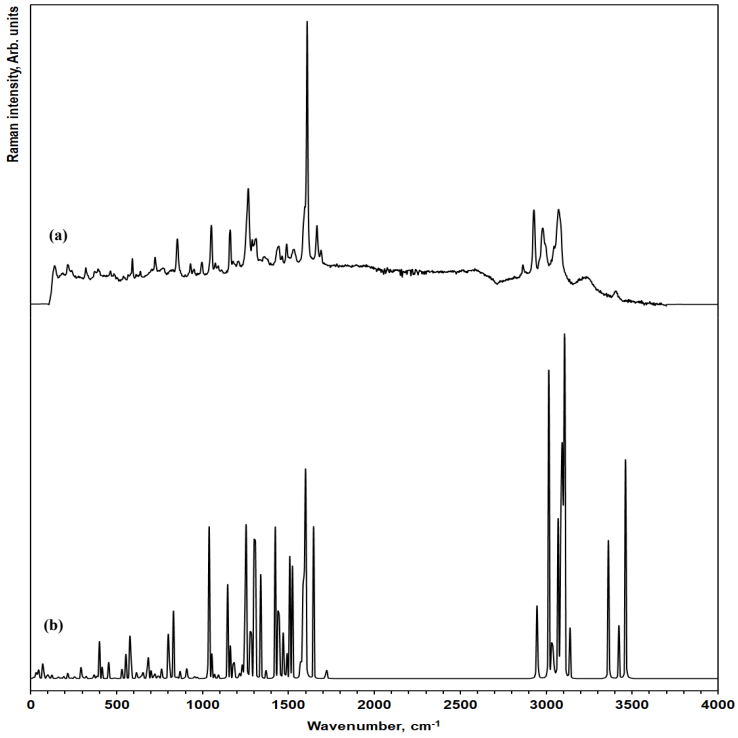

Figure 2. Experimental (a) and theoretical (b) FT-RAMAN spectrum of L^{NNN} compound.

Nicolet Spectrometer 6700 was used to record the FT-RAMAN spectrum of the title compound in the range of 4000-50 cm^{-1} at room temperature. The wavelength of the used laser was 780 nm. Figure 2 demonstrates the recorded FT-RAMAN spectrum of the title compound.

2.2. Synthesis

The solvents and chemicals used in the study were commercially obtained from Merck, Sigma-Aldrich and Alfa-Aesar companies and were used without further purification. Precursor materials *bis*(2-nitrophenyl)amine and *bis*(2-aminophenyl)amine were prepared according to the previously published method (Scheme 1) [24-28].

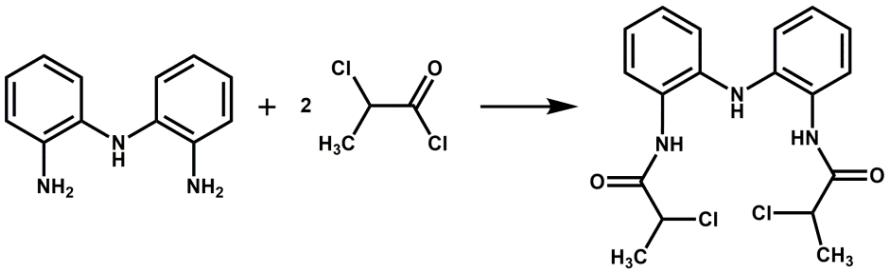

Scheme 1

A solution of 2-chloropropionyl chloride (5 mmol) in acetonitrile (50 mL) was cooled to 0 °C under nitrogen atmosphere. Then, *bis*(2-aminophenyl)amine (10 mmol) and triethylamine (Et_3N) (10 mmol) was slowly added to this cold solution over 3 h. The mixture was stirred at 0 °C for 1 hr and the mixture temperature were allowed to slowly rise to room temperature. Then, the mixture was stirred again at room temperature for 24 h and the solvent was removed under vacuum. The resulting solid was crystallized from dichloro methane/*n*-hexane mixture (1:1, *v*:*v*) (Scheme 1) [25,26]. *N,N'*-(Azanediyl*bis*(2, 1-phenylene))*bis*(2-chloropropanamide) (L^{NNN}): Color: White. Yield: 65%. ^{1}H NMR (400 MHz, $CDCl_3$, δ, ppm): 8.51 (s, 2H, NH(CO)), 7.69 (dd, 2H, Ar-H), 7.13 (td, 2H, Ar-H), 7.07 (m, 2H, Ar-H), 6.91 (dd, 2H, Ar-H), 5.74 (s, 1H, NH), 4.53 (q, 2H, CH), 1.71 (d, 6H, CH_3). ^{13}C NMR (100 MHz, $CDCl_3$, δ, ppm): 168.30 (CO), 136.00 (Ar-C), 128.43 (Ar-C), 126.89 (Ar-C), 123.90 (Ar-C), 121.31 (Ar-C), 55.90 (CH), 22.44 (CH_3), 22.41 (CH_3). FT-IR (ATR, cm^{-1}): 3397, 3099, 3060, 2980, 1690, 1662, 1651. LC-MS (+ESI, *m/z*): 380.2 $[M+H]^+$, 279.2, 242.3, 130.2, 102.2.

2.3. Calculation details

The theoretical calculations were carried out with the Gaussian 16W program packages [29]. The calculated results were visualized by means of GaussView 6.0 [30]. In the present work, we have calculated the vibrational frequencies and the geometric parameters of *N,N'*-(azanediyl*bis*(2,1-phenylene))*bis*(2-chloropropanamide) in the ground state to compare the fundamentals from the experimental vibration frequencies and geometric parameters, by using the Hartree-Fock (HF) [31], the Density functional theory using Becke's three parameter hybrid functionals [32] with Lee, Yang, and Parr correlation functional methods (B3LYP) [33], Becke's exchange functional in combination with the Lee, Yang and Parr correlation functional methods (BLYP) [32,33], the Barone and Adamo's Becke-style one-parameter functional using the modified Perdew-Wang exchange and Perdew-Wang 91 correlation method (mPW1PW91) [34,35], Becke's three parameter exchange functionals with Perdew-Wang exchange functional with Perdew and Wang's gradient correlated functional (B3PW91) [32,36] with the standard 6-31G(d,p) and 6-311G(d,p) basic sets. The frequency values computed at these levels contain known systematic errors [37]. Scaling factor values of 0.9614, 0.9679, 0.9573, 0.9631, 0.9945, 0.9934, 0.9500, 0.9567 0.8992 and 0.9051 for B3LYP/6-31G(d,p), B3LYP/6-311G(d,p), B3PW91/6-31G(d,p), B3PW91/6-311G(d,p), BLYP/6-31G(d,p), BLYP/6-311G(d,p), mPW1 PW91/6-31G(d,p), mPW1PW91/6-311G(d,p), HF/6-31G(d,p) and HF/6-311G(d,p), respectively, can be used to correct these discrepancies [38-44]. Also, optimal scaling factors were calculated for all analyzed methods. The GaussView 6.0 graphical interface of the Gaussian program, which is an animation option that provides a visual representation of the shape of the modes of vibration, provides a way of assigning the calculated wavenumbers [30]. The SQM procedure has been widely used in the assignment of bands of vibrational spectra due to being a highly successful and well established technique in refining the computerized vibration frequencies to better match the experimental values [45]. So, the vibrational modes were determined according to the potential energy distribution analysis using the SQM program [46]. Using the PAVF 1.0 program, the performance of the used method was quantitatively characterized [47]. The population analysis has also been performed by the natural bond orbital method [48] at B3LYP, BLYP, B3PW91, mPW1PW91 and HF/6-31G(d,p) and 6-311G(d,p) level of theory using the natural bond orbital (NBO) program [49] under the Gaussian 16W program package.

2.4. Hirshfeld surfaces analysis

Analysis of Hirshfeld surfaces and their associated two dimensional fingerprint plots of L^{NNN} compound were calculated by using the CrystalExplorer17 [50]. The Hirshfeld surfaces are mapped with different properties d_{norm}, shape index and curvedness. The d_{norm} is a normalized contact distance, defined in terms of d_e, d_i and the vdW radii of the atoms. The combination of d_e and d_i in the form of a 2D fingerprint plot displays the summary of intermolecular contacts in the crystal.

3. Results and discussion

3.1. Molecular geometry

The molecular structure of *N,N'*-(azanediyl*bis*(2,1-phenylene))*bis*(2-chloropropanamide) obtained by the single crystal X-ray diffraction method has been previously reported [25,26]. The compound crystallizes triclinic, space group *P*-1 (no. 2), a = 9.4053(6) Å, b = 10.8925(8) Å, c = 18.5490(13) Å, α = 76.134(2)°, β = 80.859(2)°, γ = 79.963(2)°, V = 1803.0(2) Å^3, Z = 4, T = 99.99 K, μ(MoKα) = 0.377 mm^{-1}, *Dcalc* = 1.401 g/cm^3, 149948 reflections measured (5.956° ≤ 2Θ ≤ 50.238°), 6409 unique (R_{int} = 0.1130, R_{sigma} = 0.0328) which were used in all calculations. The final R_1 was 0.0411 (I > 2σ(I)) and wR_2 was 0.0989 (all data). The optimized geometry parameters were performed by theoretical calculations using the HF and DFT (B3LYP, BLYP, B3PW91, mPW1PW91) methods with 6-31G(d,p) and 6-311G(d,p) basis sets. Full geometry optimization of structure was carried out without any restrictions. The stability of the optimized geometries was confirmed by the absence of imaginary frequencies in the vibrational spectra. The title compound belongs to C_1 point group symmetry. The comparative optimized structural parameters such as bond lengths and bond angles are presented in Table 1 in accordance with the atom numbering scheme illustrated in Figure 3. In addition, the correlation values of theoretical and experimental geometric parameters are presented at the end of Table 1.

Table 1. Optimized and experimental geometries of H_3L^{NNN} molecule in the ground state *.

Parameter	Experimental, Å	Calculated, Å									
		B3LYP		B3PW91		BLYP		mPW1PW		HF	
		6-31	6-311	6-31	6-311	6-31	6-311	6-31	6-311	6-31	6-311
Bond lengths											
C1-C2	1.505(15)	1.516	1.514	1.512	1.510	1.525	1.523	1.509	1.508	1.515	1.514
C2-Cl3	1.778(8)	1.847	1.845	1.825	1.825	1.880	1.879	1.820	1.818	1.814	1.817
C2-C4	1.520(3)	1.538	1.537	1.535	1.533	1.550	1.549	1.532	1.530	1.530	1.529
C4-O5	1.219(3)	1.222	1.214	1.220	1.213	1.235	1.228	1.217	1.210	1.195	1.189
C4-N6	1.345(3)	1.373	1.373	1.369	1.369	1.388	1.388	1.366	1.366	1.357	1.358
N6-C7	1.426(3)	1.417	1.416	1.410	1.410	1.425	1.425	1.408	1.407	1.418	1.418
C7-C8	1.385(3)	1.401	1.401	1.401	1.399	1.415	1.412	1.397	1.397	1.389	1.388
C7-C12	1.404(3)	1.417	1.412	1.412	1.409	1.427	1.425	1.411	1.407	1.397	1.395
C8-C9	1.385(3)	1.392	1.389	1.389	1.387	1.401	1.398	1.388	1.385	1.381	1.379
C9-C10	1.385(3)	1.394	1.393	1.394	1.391	1.406	1.403	1.391	1.389	1.385	1.385
C10-C11	1.382(3)	1.391	1.388	1.388	1.386	1.400	1.397	1.387	1.384	1.380	1.379
C11-C12	1.393(3)	1.403	1.398	1.399	1.396	1.412	1.410	1.399	1.394	1.393	1.392
C12-N13	1.399(3)	1.407	1.416	1.411	1.410	1.427	1.425	1.399	1.409	1.403	1.405
N13-C14	1.397(3)	1.398	1.414	1.409	1.408	1.425	1.423	1.390	1.405	1.399	1.402
C14-C15	1.392(3)	1.407	1.398	1.399	1.396	1.412	1.409	1.402	1.393	1.393	1.392
C14-C19	1.406(3)	1.415	1.413	1.413	1.411	1.428	1.425	1.410	1.409	1.398	1.397
C15-C16	1.381(3)	1.392	1.391	1.392	1.389	1.403	1.400	1.388	1.388	1.383	1.383
C16-C17	1.383(3)	1.396	1.393	1.394	1.391	1.406	1.403	1.392	1.389	1.384	1.383
C17-C18	1.379(3)	1.392	1.391	1.392	1.389	1.403	1.400	1.388	1.388	1.383	1.382
C18-C19	1.390(3)	1.395	1.396	1.397	1.394	1.410	1.407	1.391	1.392	1.383	1.382
C19-N20	1.425(3)	1.424	1.416	1.410	1.409	1.425	1.426	1.416	1.407	1.421	1.421
N20-C21	1.344(3)	1.351	1.346	1.343	1.343	1.359	1.360	1.345	1.340	1.339	1.339
C21-O22	1.222(2)	1.237	1.235	1.239	1.233	1.256	1.248	1.232	1.230	1.210	1.205
C21-C23	1.518(3)	1.534	1.535	1.531	1.530	1.547	1.546	1.527	1.527	1.527	1.527
C23-C24	1.514(10)	1.528	1.525	1.523	1.520	1.537	1.535	1.521	1.518	1.526	1.524
C23-Cl25	1.813(3)	1.835	1.834	1.814	1.815	1.866	1.869	1.809	1.808	1.803	1.806
C26-C27	1.537(15)	1.516	1.514	1.512	1.510	1.525	1.523	1.509	1.508	1.515	1.514
C27-Cl28	1.756(5)	1.847	1.845	1.825	1.825	1.880	1.879	1.820	1.818	1.814	1.817
C27-C29	1.517(3)	1.538	1.537	1.535	1.533	1.550	1.549	1.532	1.530	1.530	1.529
C29-O30	1.226(2)	1.222	1.214	1.220	1.213	1.235	1.228	1.217	1.210	1.195	1.189
C29-N31	1.352(3)	1.373	1.373	1.369	1.369	1.388	1.388	1.366	1.366	1.357	1.358
N31-C32	1.428(3)	1.417	1.416	1.410	1.410	1.425	1.425	1.408	1.407	1.418	1.418
C32-C33	1.385(3)	1.401	1.401	1.401	1.399	1.415	1.412	1.397	1.397	1.389	1.388
C32-C37	1.401(3)	1.417	1.412	1.412	1.409	1.427	1.425	1.411	1.407	1.397	1.395
C33-C34	1.386(3)	1.392	1.389	1.389	1.387	1.401	1.398	1.388	1.385	1.381	1.379
C34-C35	1.375(3)	1.394	1.393	1.394	1.391	1.406	1.403	1.391	1.389	1.385	1.385
C35-C36	1.386(3)	1.391	1.388	1.388	1.386	1.400	1.397	1.387	1.384	1.380	1.379
C36-C37	1.393(3)	1.403	1.398	1.399	1.396	1.412	1.410	1.399	1.394	1.393	1.392
C37-N38	1.400(3)	1.407	1.416	1.411	1.410	1.427	1.425	1.399	1.409	1.403	1.405
N38-C39	1.400(3)	1.398	1.414	1.409	1.408	1.425	1.423	1.390	1.405	1.399	1.402
C39-C40	1.397(3)	1.407	1.398	1.399	1.396	1.412	1.409	1.402	1.393	1.393	1.392
C39-C44	1.398(3)	1.415	1.413	1.413	1.411	1.428	1.425	1.410	1.409	1.398	1.397
C40-C41	1.380(3)	1.392	1.391	1.392	1.389	1.403	1.400	1.388	1.388	1.383	1.383
C41-C42	1.383(3)	1.396	1.393	1.394	1.391	1.406	1.403	1.392	1.389	1.384	1.383
C42-C43	1.385(3)	1.392	1.391	1.392	1.389	1.403	1.400	1.388	1.388	1.383	1.382
C43-C44	1.385(3)	1.395	1.396	1.397	1.394	1.410	1.407	1.391	1.392	1.383	1.382
C44-N45	1.427(3)	1.424	1.416	1.410	1.409	1.425	1.426	1.416	1.407	1.421	1.421
N45-C46	1.336(3)	1.351	1.346	1.343	1.343	1.359	1.360	1.345	1.340	1.339	1.339
C46-O47	1.218(3)	1.237	1.235	1.239	1.233	1.256	1.248	1.232	1.230	1.210	1.205
C46-C48	1.514(3)	1.534	1.535	1.531	1.530	1.547	1.546	1.527	1.527	1.527	1.527
C48-C49	1.554(15)	1.528	1.525	1.523	1.520	1.537	1.535	1.521	1.518	1.526	1.524
C48-Cl50	1.766(6)	1.835	1.834	1.814	1.815	1.866	1.869	1.809	1.808	1.803	1.806
r		0.9931	0.9929	0.9932	0.9933	0.9901	0.9906	0.9939	0.9936	0.9962	0.9959
Bond angles											
C1-C2-Cl3	111.30(11)	109.99	109.93	110.17	110.11	109.69	109.66	110.23	110.17	110.23	110.15
C1-C2-C4	114.80(10)	111.90	112.18	111.63	111.95	112.12	112.41	111.60	111.85	112.18	112.43
Cl3-C2-C4	108.80(4)	108.11	107.20	107.36	107.16	107.25	107.19	108.25	107.10	108.25	108.04
C2-C4-O5	123.34(19)	121.12	121.27	121.20	121.37	121.26	121.40	121.18	121.37	121.04	121.20
C2-C4-N6	113.48(17)	113.65	113.38	113.49	113.24	113.47	113.29	113.53	113.23	114.13	113.84
O5-C4-N6	123.20(2)	125.21	125.35	125.31	125.39	125.27	125.30	125.27	125.40	124.81	124.94
C4-N6-C7	125.14(17)	125.92	126.70	126.52	126.67	126.98	126.98	125.67	126.57	124.34	124.54
N6-C7-C8	121.42(19)	121.88	122.00	122.03	122.07	122.00	121.94	121.92	122.15	120.96	121.00
N6-C7-C12	118.37(18)	118.62	118.76	118.73	118.71	118.83	118.88	118.54	118.61	119.18	119.20
C8-C7-C12	120.21(19)	119.50	119.23	119.23	119.22	119.16	119.18	119.53	119.24	119.86	119.79
C7-C8-C9	120.80(2)	120.67	120.53	120.52	120.53	120.55	120.60	120.65	120.45	120.77	120.79
C8-C9-C10	119.10(2)	120.01	120.32	120.34	120.33	120.38	120.30	120.00	120.38	119.56	119.59
C9-C10-C11	120.70(2)	119.90	119.61	119.59	119.59	119.61	119.67	119.91	119.58	120.15	120.06
C10-C11-C12	120.70(2)	121.01	121.01	120.98	120.98	121.04	121.07	120.96	120.91	120.87	120.92
C7-C12-C11	118.45(19)	118.89	119.27	119.31	119.32	119.22	119.14	118.94	119.40	118.78	118.84
C7-C12-N13	117.71(18)	120.11	121.32	121.36	121.25	121.54	121.39	120.03	121.14	120.29	120.50
C11-C12-N13	123.79(19)	120.93	119.38	119.30	119.41	119.19	119.43	120.97	119.43	120.86	120.60
C12-N13-C14	129.42(18)	126.37	122.60	122.19	122.37	122.73	123.35	126.03	122.12	125.19	124.64
N13-C14-C15	123.90(19)	123.11	123.12	123.14	123.12	123.05	122.95	123.14	123.22	123.37	123.38
N13-C14-C19	117.80(18)	118.93	118.10	118.03	118.05	118.22	118.37	118.85	117.91	118.46	118.40
C15-C14-C19	118.24(19)	117.95	118.78	118.83	118.83	118.73	118.68	118.00	118.86	118.16	118.22
C14-C15-C16	120.50(2)	120.81	120.66	120.58	120.62	120.63	120.70	120.77	120.58	120.76	120.80
C15-C16-C17	121.10(2)	120.69	120.16	120.15	120.15	120.20	120.21	120.70	120.17	120.61	120.54

Table 1. Continued.

Parameter	Experimental, Å	Calculated, Å									
		B3LYP		B3LYP		B3LYP		B3LYP		B3LYP	
		6-31	6-311	6-31	6-311	6-31	6-311	6-31	6-311	6-31	6-311
Bond angles											
C16-C17-C18	119.20(2)	119.30	120.11	120.18	120.13	120.19	120.09	119.30	120.14	119.18	119.18
C17-C18-C19	120.50(2)	120.47	120.00	119.91	119.98	119.93	120.06	120.44	119.94	120.58	120.63
C14-C19-C18	120.49(19)	120.76	120.23	120.28	120.22	120.25	120.21	120.78	120.24	120.67	120.60
C14-C19-N20	119.26(18)	118.36	116.27	116.06	116.12	116.32	116.62	118.22	115.95	118.54	118.48
C18-C19-N20	120.25(19)	120.85	123.44	123.59	123.60	123.34	123.08	120.97	123.76	120.76	120.89
C19-N20-C21	123.45(17)	125.56	129.11	129.06	129.21	129.30	129.20	125.38	129.18	124.94	125.13
N20-C21-O22	123.60(2)	124.24	124.80	124.64	124.81	124.63	124.85	124.18	124.76	124.51	124.62
N20-C21-C23	114.63(18)	118.02	117.90	117.91	117.65	117.97	117.83	117.91	117.67	118.28	118.21
O22-C21-C23	122.76(19)	117.69	117.29	117.43	117.53	117.36	117.29	117.87	117.57	117.11	117.09
C21-C23-C24	112.30(5)	111.32	111.45	111.08	111.32	111.70	111.87	110.99	111.28	110.48	110.73
C21-C23-Cl25	110.46(16)	113.30	113.68	113.79	113.72	113.37	113.55	113.42	113.70	113.79	113.73
C24-C23-Cl25	110.70(5)	109.71	109.57	109.80	109.68	109.48	109.28	109.92	109.70	110.06	109.93
C26-C27-Cl28	107.00(10)	109.99	109.93	110.17	110.11	109.69	109.66	110.23	110.17	110.23	110.15
C26-C27-C29	105.50(9)	111.90	112.18	111.63	111.95	112.12	112.41	111.60	111.85	112.18	112.43
Cl28-C27-C29	109.90(3)	108.11	107.20	107.36	107.16	107.25	107.19	108.25	107.10	108.26	108.04
C27-C29-O30	122.12(19)	121.12	121.26	121.20	121.37	121.26	121.40	121.18	121.37	121.04	121.20
C27-C29-N31	114.45(18)	113.65	113.38	113.49	113.24	113.47	113.29	113.53	113.23	114.13	113.84
O30-C29-N31	123.40(2)	125.21	125.35	125.31	125.39	125.27	125.30	125.27	125.40	124.81	124.94
C29-N31-C32	123.35(17)	125.92	126.70	126.52	126.67	126.98	126.98	125.67	126.57	124.34	124.54
N31-C32-C33	119.61(18)	121.88	122.00	122.03	122.07	122.00	121.94	121.92	122.15	120.96	121.00
N31-C32-C37	119.55(18)	118.62	118.77	118.73	118.71	118.83	118.88	118.54	118.61	119.17	119.20
C33-C32-C37	120.84(19)	119.50	119.23	119.23	119.22	119.16	119.18	119.53	119.24	119.86	119.79
C32-C33-C34	120.30(2)	120.67	120.53	120.52	120.53	120.55	120.60	120.65	120.45	120.77	120.79
C33-C34-C35	119.30(2)	120.01	120.32	120.34	120.33	120.38	120.30	120.00	120.38	119.56	119.59
C34-C35-C36	121.00(2)	119.90	119.61	119.59	119.59	119.61	119.67	119.91	119.58	120.15	120.06
C35-C36-C37	120.50(2)	121.01	121.01	120.98	120.98	121.04	121.07	120.96	120.91	120.87	120.92
C32-C37-C36	118.07(19)	118.89	119.27	119.31	119.32	119.22	119.14	118.94	119.40	118.78	118.84
C32-C37-N38	117.71(18)	120.11	121.32	121.36	121.25	121.54	121.39	120.03	121.14	120.29	120.50
C36-C37-N38	124.20(2)	120.93	119.38	119.30	119.41	119.19	119.43	120.97	119.43	120.86	120.60
C37-N38-C39	128.16(18)	126.37	122.59	122.19	122.37	122.73	123.35	126.03	122.12	125.19	124.63
N38-C39-C40	123.80(2)	123.11	123.12	123.14	123.12	123.05	122.95	123.14	123.22	123.37	123.38
N38-C39-C44	118.17(19)	118.93	118.11	118.03	118.05	118.22	118.37	118.85	117.92	118.46	118.40
C40-C39-C44	118.00(2)	117.95	118.78	118.83	118.83	118.73	118.68	118.00	118.86	118.16	118.22
C39-C40-C41	120.60(2)	120.81	120.66	120.58	120.62	120.63	120.70	120.77	120.58	120.76	120.80
C40-C41-C42	121.00(2)	120.69	120.16	120.16	120.15	120.20	120.21	120.70	120.17	120.61	120.54
C41-C42-C43	119.10(2)	119.30	120.11	120.18	120.13	120.19	120.09	119.30	120.14	119.18	119.18
C42-C43-C44	120.30(2)	120.47	120.00	119.91	119.98	119.93	120.06	120.44	119.94	120.58	120.63
C39-C44-C43	121.10(2)	120.76	120.23	120.28	120.22	120.25	120.21	120.78	120.24	120.67	120.60
C39-C44-N45	118.91(18)	118.36	116.27	116.06	116.12	116.32	116.62	118.22	115.95	118.54	118.48
C43-C44-N45	120.00(2)	120.85	123.44	123.59	123.60	123.34	123.08	120.97	123.76	120.76	120.89
C44-N45-C46	122.10(17)	125.56	129.11	129.06	129.21	129.30	129.20	125.38	129.18	124.94	125.13
N45-C46-O47	122.10(2)	124.24	124.80	124.65	124.81	124.63	124.85	124.18	124.76	124.51	124.62
N45-C46-C48	115.30(18)	118.02	117.90	117.91	117.65	117.97	117.83	117.91	117.67	118.28	118.21
O47-C46-C48	122.50(2)	117.69	117.29	117.43	117.53	117.36	117.29	117.87	117.57	117.11	117.09
C46-C48-C49	110.70(10)	111.32	111.45	111.08	111.32	111.70	111.87	110.99	111.28	110.48	110.73
C46-C48-Cl50	110.20(3)	113.30	113.68	113.79	113.72	113.37	113.55	113.42	113.70	113.79	113.73
C49-C48-Cl50	111.60(11)	109.71	109.57	109.80	109.68	109.48	109.28	109.92	109.70	110.06	109.93
r		0.9175	0.8450	0.8419	0.8444	0.8451	0.8525	0.9192	0.8424	0.9101	0.9035

* 6-31: 6-31G(d,p); 6-311: 6-311G(d,p); The atom numbering scheme given in Figure 3(a).

On Table 1, it can be seen that, the theoretical and experimental structure parameters obtained in this study were found to be both in harmony with each other and experimental one. In the bond length calculations, the best correlation (r = 0.9962) was found for the HF/6-31G(d,p) method, and the maximum difference between the theoretical and experimental bond lengths (C27-Cl28) was 0.058 Å. In the bond angle calculations, the best correlation (r = 0.9192) was found for the mPW1PW91/6-31G(d,p) method, and the maximum difference between the theoretical and experimental bond angles (C26-C27-C29) was 6.10°. We discovered some minor differences between the experimental (solid phase) and the theoretical (gas phase) structure parameters of the title compound. The experimental structure parameters of title compound are obtained from solid phase and it is clear, that the solid phase of the compounds includes various crystal interactions [25,26,39-44].

3.2. Vibrational assignments

The theoretical calculations were performed to obtain the harmonic frequencies, RAMAN activities and IR intensities required for the vibrational assignment of the experimental spectra of the title compound. The theoretical values were calculated via the HF and DFT (B3LYP, B-LYP, B3PW91, mPW1PW91) methods with the 6-31G (d, p) and 6-311G(d, p) basis sets. The title compound molecule possesses no symmetry elements and belongs to the C_1 point group symmetry. The title molecule consists of 88 (2×44) atoms, which undergo 258 normal modes of vibration. The calculated frequencies, measured RAMAN and IR band positions and their assignments along with corresponding potential energy distribution (PED) contributions are summarized in Table 2. Based on the normal coordinate analysis (NCA) IR and RAMAN spectral wavenumbers have been assigned. The vibrational assignments for different functional groups have been discussed below. The recorded FT-IR and FT-RAMAN spectra of the compound are also presented with the calculated frequencies in Figure 1 and 2, respectively. The vibrational band assignments have been made by using both the animation option of the GaussView 6.0 graphical interface for the Gaussian 16W program [29,30] and the SQM 2.0 program [46]. All the calculated spectra were found to be in good accordance with the experimental ones. Considering Table 2, it can be concluded that experimental bases better aligned with the scaled fundamentals and have a better correlation with B3LYP/6-31G(d,p) than the other calculation methods.

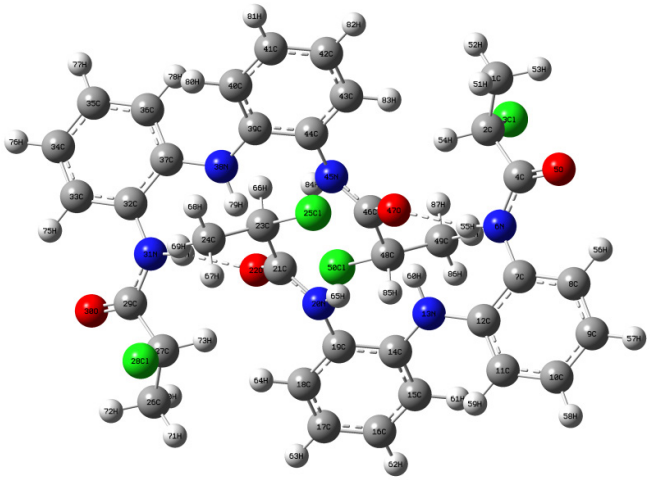

(a)

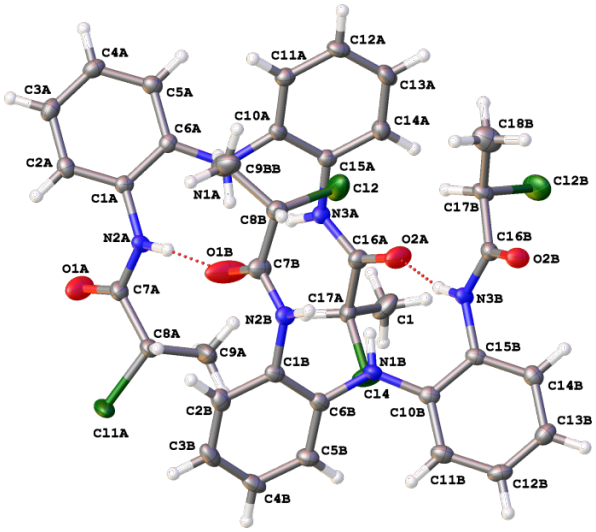

(b)

Figure 3. The optimized geometry of L^{NNN} molecule calculated at B3LYP/6-31G(d,p) level (a) and a view of the molecular structure of L^{NNN} molecule with displacement ellipsoids drawn at the 50% probability level [25] (b).

Overall better performance of the used calculation methods can be quantitatively characterized by using the mean absolute percentage error, mean absolute error, root mean square values (RMS) and coefficients of correlation (*r*) between the theoretically calculated and experimentally observed vibration frequencies (Table 3). All these values were calculated in this study by the PAVF 1.0 program [47] according to Scott and Radom [38]. The *r* values for all DFT methods were greater than 0.9993. We calculated the optimal scaling factors, which are crucial for IR spectral predictions, using the PAVF 1.0 program [47]. Without accounting for different vibrations, only single-uniform scaling factors were calculated. The values obtained are 0.9615, 0.9675, 0.9595, 0.9647, 0.9922, 0.9970, 0.9524, 0.9585, 0.9023 ve 0.9078 for the B3LYP/6-31G(d,p), B3LYP/6-311G(d,p), B3PW91/6-31G(d,p), B3PW91/6-311G(d,p), B-LYP/6-31G(d,p), B-LYP/6-311G(d,p), mPW1PW91/6-31G(d,p), mPW1PW91/6-311G (d,p), HF/6-31G(d,p) and HF/6-311G(d,p), methods, respectively. They are very close to those recommended by Scott and Radom [47] for the same level of theory.

The N-H stretching vibrations of aromatic amines arise in the range of 3340-3520 cm^{-1} [51]. The symmetric and anti-symmetric stretching modes (Observed: 3413, 3404, 3397 cm^{-1}, Calculated: 3462, 3422, 3363 cm^{-1}) are assigned in the spectra of the title compound in the appropriate range. The difference between calculated and observed N-H stretching modes can be explained by the hydrogen bonds which occur in the solid phase.

The C=O stretching vibrations arise in the region 1710-1680 cm^{-1} [52]. In the IR spectrum of title compound, the C=O stretching vibrations are found at 1690, 1662 and 1651 cm^{-1} and were calculated at 1720, 1656 and 1646 cm^{-1}.

In general, an aromatic C-H stretching vibrations occurs in the region 3100-3000 cm^{-1} [53-55] and they are affected by the nature of substituent. The title compound has two aromatic groups which have eight C-H adjacent moieties. These C-H stretching modes contributed to five different bands in the RAMAN spectrum of the title compound, located at 3136, 3109, 3092, 3074 and 3069 cm^{-1} and five bands in the IR spectrum at 3136, 3118, 3099, 3076 and 3060 cm^{-1} which were in agreement with the calculated ones. The PED contribution of these stretching modes was calculated as 73-100%, meaning that these local coordinates fully explain the C-H aromatic vibration modes.

The symmetric (ν_sCH_3) and asymmetric ($\nu_{as}CH_3$) stretching modes are usually observed in the range between 3050 and 2950 cm^{-1} [56]. Our theoretical calculations for the title compound locate these modes for methyl group at the following wavenumbers: $\nu_{as}CH_3$: 3048, 3036, 3029, 3016 and 3015, and ν_sCH_3: 3013, 2949 and 2944 cm^{-1}. They agree well with the experimental values (Table 2).

Table 2. Vibrational wavenumbers obtained for L^{NNN} at 6-31G(d,p) level.

No	Exp. IR (cm^{-1})	RAMAN (cm^{-1})	B3LYP					Assignments, PED (%)
			Unscaled (cm^{-1})	Scaled (cm^{-1})	Scaled (cm^{-1})	IR Int. (km/mol)	RAMAN activity (A^4/amu)	
1	3413	3407	3601	3462	3462	165.36	0.01	νNH_{ring}, 100
2	3413	3407	3601	3462	3462	0.01	572.86	νNH_{ring}, 97
3	3404	3407	3559	3421	3422	0.01	166.41	νNH_{Carb}, 97
4	3404	3407	3558	3421	3422	135.07	0.01	νNH_{Carb}, 96
5	3397	3397	3498	3363	3363	709.45	0.02	νNH_{Carb}, 90
6	3397	3397	3497	3362	3363	0.03	462.97	νNH_{Carb}, 91
7	3136	3136	3263	3137	3137	0.22	140.03	νCH_{arom}, 100, sym
8	3136	3136	3263	3137	3137	2.26	13.35	νCH_{arom}, 99, sym
9	3118	3109	3232	3108	3108	2.28	2.11	νCH_{arom}, 89, sym
10	3118	3109	3232	3108	3108	0.01	399.95	νCH_{arom}, 88, sym
11	3099	3092	3224	3100	3100	9.00	0.05	νCH_{arom}, 83, sym
12	3099	3092	3224	3100	3100	0.01	176.26	νCH_{arom}, 82, sym
13	3099	3092	3216	3092	3092	16.18	0.01	νCH_{arom}, 83, sym
14	3099	3092	3216	3092	3092	0.01	237.82	νCH_{arom}, 82, sym
15	3076	3074	3209	3085	3086	0.01	279.89	νCH_{arom}, 77, asym
16	3076	3074	3209	3085	3086	29.47	0.01	νCH_{arom}, 77, asym
17	3076	3074	3205	3082	3082	0.01	436.27	νCH_{arom}, 73, asym
18	3076	3074	3205	3082	3082	54.32	0.01	νCH_{arom}, 73, asym
19	3060	3069	3192	3068	3069	0.01	166.92	νCH_{arom}, 78, asym
20	3060	3069	3192	3068	3069	9.19	0.07	νCH_{arom}, 78, asym
21	3060	3069	3189	3066	3066	5.63	0.02	νCH_{arom}, 83, asym
22	3060	3069	3189	3066	3066	0.01	140.03	νCH_{arom}, 83, asym
23	3045	3045	3171	3048	3049	11.23	0.01	νCH_{metil}, asym, 80 + νCH, 15
24	3045	3045	3171	3048	3048	0.01	81.72	νCH_{metil}, asym, 80 + νCH, 15
25	3045	3045	3158	3036	3037	10.60	0.04	νCH_{metil}, asym, 44 + νCH, 43
26	3045	3045	3158	3036	3037	0.01	128.03	νCH, 44 + νCH_{metil}, asym, 43
27	3045	3045	3151	3029	3029	0.01	95.64	νCH_{metil}, asym, 80 + νCH, 17
28	3045	3045	3151	3029	3029	9.61	0.01	νCH_{metil}, asym, 80 + νCH, 17
29	3018	3029	3137	3016	3016	23.02	0.01	νCH_{metil}, asym, 78 + νCH, 13
30	3018	3029	3137	3016	3016	0.01	191.34	νCH_{metil}, asym, 78 + νCH, 13
31	3018	3020	3136	3015	3015	0.01	175.43	νCH_{metil}, asym, 56 + νCH, 23
32	3018	3020	3136	3015	3015	7.24	0.11	νCH, 45 + νCH_{metil}, asym, 34
33	3018	3020	3134	3013	3013	8.02	1.70	νCH_{metil}, sym, 73 + νCH, 18
34	3018	3020	3134	3013	3013	0.04	308.73	νCH_{metil}, sym, 72 + νCH, 18
35	2980	2982	3067	2949	2949	0.01	213.32	νCH_{metil}, sym, 76
36	2980	2982	3067	2949	2949	13.4	0.17	νCH_{metil}, sym, 76
37	2927	2929	3062	2944	2944	19.44	0.01	νCH_{metil}, sym, 71
38	2927	2929	3062	2944	2944	0.01	213.99	νCH_{metil}, sym, 71
39	1690	1691	1789	1720	1720	0.01	72.49	νCO, 71
40	1690	1691	1789	1720	1720	457.77	0.01	νCO, 73
41	1662	1666	1723	1656	1656	855.44	0.01	νCO, 74
42	1651	1651	1712	1646	1646	0.01	119.58	νCO, 73
43	1597	1608	1663	1599	1599	33.23	0.01	νCC_{arom}, 86
44	1597	1608	1662	1598	1598	0.01	635.52	νCC_{arom}, 96
45	1593	1594	1657	1593	1593	0.01	132.25	νCC_{arom}, 72 + δCNH, 12
46	1593	1594	1656	1592	1593	340.93	0.01	νCC_{arom}, 76 + δCNH, 14
47	1589	1584	1651	1587	1587	77.99	0.01	νCC_{arom}, 56 + δCNH, 25
48	1589	1584	1649	1586	1586	0.01	177.08	νCC_{arom}, 81 + δCNH, 10
49	1576	1582	1637	1573	1573	62.71	0.01	νCC_{arom}, 75 + δCNH, 11
50	1576	1582	1636	1573	1573	0.01	161.34	νCC_{arom}, 78 + δCNH, 10
51	1524	1531	1585	1524	1524	474.82	0.01	δCNH, 48 + νCC_{arom}, 21
52	1524	1531	1584	1523	1523	0.01	80.12	δCNH 47 + νCC_{arom}, 20
53	1518	1520	1574	1513	1513	591.1	0.01	νNC_{Carb}, 41 + δCNH, 31 + νCC_{arom}, 17
54	1518	1520	1569	1508	1508	0.01	140.82	νNC_{Carb}, 42 + δCNH, 30 + νCC_{arom}, 14
55	1506	1489	1550	1490	1491	0.01	68.76	δCNH, 58 + δNCH, 26 + νCC_{arom}, 11
56	1506	1489	1550	1490	1490	786.90	0.01	δCNH, 57 + δNCH, 18 + νCC_{arom}, 11
57	1460	1463	1530	1471	1471	11.11	0.01	δCH_{arom}, ipb, 81 + δCNH, 11
58	1460	1463	1530	1471	1471	0.01	122.68	δCH_{arom}, ipb, 80 + δCNH, 11
59	1455	1450	1508	1450	1450	5.40	0.01	δCH_{metil}, scis, 59 + δCH_{arom}, ipb, 14
60	1455	1450	1508	1449	1450	0.01	26.79	δHCH_{metil}, scis, 63 + δCH_{arom}, ipb, 16
61	1447	1444	1504	1446	1446	73.93	0.01	δCH_{arom}, ipb, 69 + δHCH_{metil}, scis, 11
62	1447	1444	1504	1446	1446	0.01	46.25	δCH_{arom}, ipb, 68 + δHCH_{metil}, scis, 10
63	1440	1437	1500	1442	1442	0.01	13.56	δHCH_{metil}, scis, 48 + δCH_{arom}, ipb, 32 + δCNH, 12
64	1440	1437	1500	1442	1442	278.73	0.01	δHCH_{metil}, scis, 44 + δCH_{arom}, ipb, 35 + δCNH, 18
65	1440	1437	1499	1441	1441	62.26	0.01	δCH_{metil}, scis, 52 + δCH_{arom}, ipb, 21
66	1440	1437	1499	1441	1441	0.01	19.77	δCH_{metil}, scis, 56 + δCH_{arom}, ipb, 20
67	1436	1431	1497	1440	1440	36.64	0.01	δCH_{metil}, scis, 59 + δCH_{arom}, ipb, 14
68	1436	1431	1496	1438	1438	0.01	38.79	δCH_{metil}, scis, 48 + δCH_{arom}, ipb, 18
69	1433	1431	1494	1436	1436	0.01	25.47	δCH_{metil}, scis, 54
70	1433	1431	1494	1436	1436	37.44	0.01	δCH_{metil}, scis, 46
71	1423	1425	1480	1423	1423	0.01	113.16	δCH_{arom}, ipb, 42 + δNH, 22
72	1423	1425	1479	1422	1422	185.52	0.01	δCH_{arom}, ipb, 43 + δNH, 22
73	1374	1379	1425	1370	1371	0.01	8.34	δCH_{metil}, umbr, 79
74	1374	1379	1425	1370	1370	24.73	0.01	δCH_{metil}, umbr, 79
75	1363	1362	1423	1368	1368	4.40	0.01	δCH_{metil}, umbr, 91
76	1363	1362	1423	1368	1368	0.01	6.11	δCH_{metil}, umbr, 90
77	1331	1336	1392	1339	1339	0.01	81.98	νCC_{metil}, 27 + νCC_{Carb}, 18 + δCH_{metil}, wagg, 17 + δCH, 11
78	1331	1336	1392	1339	1339	29.00	0.01	νCC_{metil}, 26 + νCC_{Carb}, 17 + δCH_{metil}, wagg, 17 + δCH, 13

Table 2. Continued.

No	Exp. IR (cm^{-1})	RAMAN (cm^{-1})	B3LYP					Assignments, PED (%)
			Unscaled (cm^{-1})	Scaled (cm^{-1})	Scaled (cm^{-1})	IR Int. (km/mol)	RAMAN activity (A^4/amu)	
79	1321	1311	1360	1308	1308	121.43	0.01	νCC_{arom}, 66 + δCH_{arom}, ipb, 15
80	1321	1311	1360	1307	1307	0.01	110.82	νCC_{arom}, 65 + δCH_{arom}, ipb, 17
81	1289	1289	1351	1299	1299	51.96	0.01	νCC_{arom}, 44 + νCN 24 + δCH, 10
82	1289	1289	1351	1299	1299	0.01	139.64	νCC_{arom}, 45 + νCN 24 + δCH, 11
83	1289	1289	1336	1285	1285	21.35	0.01	δCH_{arom}, ipb, 70
84	1289	1289	1336	1284	1285	0.01	26.98	δCH_{arom}, ipb, 76
85	1271	1271	1331	1279	1280	137.60	0.01	δCH_{arom}, ipb, 64 + δCH, 12
86	1271	1271	1331	1279	1279	0.01	49.19	δCH_{arom}, ipb, 60 + δCH, 14
87	1265	1266	1329	1278	1278	65.77	0.01	δCH_{arom}, ipb, 41 + δCH, 34
88	1265	1266	1328	1277	1277	0.01	27.66	δCH_{arom}, ipb, 42 + δCH, 37
89	1255	1258	1303	1253	1253	107.04	0.01	δCH_{arom}, ipb, 24 + νCN, 23 + δNH, 15 + νCC_{arom}, 12
90	1255	1258	1303	1253	1253	0.01	162.52	δCH_{arom}, ipb, 25 + νCN 24 + δNH, 15 + νCC_{arom}, 14
91	1246	1246	1299	1249	1249	0.01	447.27	νNC_{arom}, 52 + δNH, 18 + δCH_{arom}, ipb, 11
92	1246	1246	1299	1248	1249	117.56	0.01	νNC_{arom}, 53 + δNH, 16 + δCH_{arom}, ipb, 11
93	1238	1238	1281	1232	1232	46.98	0.01	δHCCl, 76
94	1238	1238	1281	1232	1232	0.01	16.11	δHCCl, 76
95	1215	1220	1276	1227	1227	0.01	11.91	δHCCl, 61 + δCH_{metil}, 12
96	1215	1220	1275	1226	1226	79.13	0.01	δHCCl, 62 + δCH_{metil}, 12
97	1208	1208	1262	1214	1214	35.51	0.01	νNC_{Carb}, 61 + δNH, 16 + δCH_{arom}, ipb, 12
98	1208	1208	1261	1212	1213	0.01	26.43	νNC_{Carb}, 64 + δCH_{arom}, ipb, 15 + δNH, 15
99	1189	1191	1234	1186	1186	0.01	42.18	δCH_{arom}, ipb, 76 + δNH, 14
100	1189	1191	1234	1186	1186	73.74	0.01	δCH_{arom}, ipb, 82 + δNH, 11
101	1180	1177	1225	1177	1177	1.81	0.01	δCH_{arom}, ipb, 72 + νCC_{arom}, 11
102	1180	1177	1224	1177	1177	0.01	8.93	δCH_{arom}, ipb, 69 + νCC_{arom}, 14
103	1162	1161	1208	1162	1162	0.01	22.08	δCH_{arom}, ipb, 62 + δNH, 15 + δCH, 12
104	1162	1161	1208	1162	1162	135.30	0.01	δCH_{arom}, ipb, 59 + δNH, 10 + δCH, 10
105	1157	1158	1193	1147	1147	0.01	57.68	δCH_{arom}, ipb, 64
106	1157	1158	1193	1147	1147	2.38	0.01	δCH_{arom}, ipb, 67
107	1148	1148	1191	1145	1145	4.09	0.01	δCH_{arom}, ipb, 65
108	1148	1148	1191	1145	1145	0.01	57.25	δCH_{arom}, ipb, 66
109	1108	1109	1138	1094	1094	21.87	0.01	δCH_{arom}, ipb, 46 + δCH_{metil}, 13 + νCC, 11
110	1108	1109	1137	1094	1094	0.01	6.78	δCH_{arom}, ipb, 48 + νCC, 13 + δCH_{metil}, 12
111	1092	1091	1132	1088	1088	8.68	0.01	δCH_{arom}, ipb, 66 + νCC_{arom}, 21
112	1092	1091	1132	1088	1088	0.01	4.19	δCH_{arom}, ipb, 66 + νCC_{arom}, 22
113	1073	1074	1114	1071	1071	0.01	9.09	δCH_{arom}, ipb, 34 + νCC_{arom}, 25 + νCC, 14
114	1073	1074	1113	1070	1070	7.41	0.01	δCH_{arom}, ipb, 35 + νCC_{arom}, 26 + νCC, 12
115	1051	1051	1097	1054	1054	14.54	0.01	δCH_{metil}, wagg, 47 + δCH, 12
116	1051	1051	1097	1054	1054	0.01	14.82	δCH_{metil}, wagg, 45 + δCH, 13
117	1051	1051	1095	1053	1053	9.82	0.01	δCH_{metil}, wagg, 57 + δCH, 14
118	1051	1051	1095	1053	1053	0.01	9.73	δCH_{metil}, wagg, 53 + δCH, 18
119	1051	1051	1092	1050	1050	0.01	2.14	δCH_{metil}, wagg, 59 + δCH, 23
120	1051	1051	1092	1050	1050	39.92	0.01	δCH_{metil}, wagg, 58 + δCH, 21
121	1040	1039	1080	1039	1039	0.01	112.10	νCC_{arom}, ring breating, 66 + δCH_{arom}, ipb, 24
122	1040	1039	1080	1039	1039	21.54	0.01	νCC_{arom}, ring breating, 65 + δCH_{arom}, ipb, 23
123	1037	1039	1074	1032	1032	0.01	28.78	νCC_{arom}, ring breating, 57 + δCH_{arom}, ipb, 18
124	1037	1039	1074	1032	1032	7.81	0.01	νCC_{arom}, ring breating, 56 + δCH_{arom}, ipb, 19
125	995	996	1006	967	967	26.92	0.01	δCH, 56 + δCH_{metil}, wagg, 23
126	995	996	1006	967	967	0.01	4.63	δCH, 54 + δCH_{metil}, wagg, 25
127	968	968	995	956	957	28.97	0.01	νCC, 27 + δCH_{metil}, wagg, 19 + δCH, 18
128	968	968	994	956	956	0.01	7.66	νCC, 28 + δCH_{metil}, wagg, 19 + δCH, 16
129	950	951	986	948	948	0.01	1.42	δCH_{arom}, opb, 60
130	950	951	986	948	948	1.31	0.01	δCH_{arom}, opb, 59
131	942	943	978	940	940	0.01	0.41	δCH_{arom}, opb, 65
132	942	943	978	940	940	2.58	0.01	δCH_{arom}, opb, 65
133	925	929	965	928	928	2.47	0.01	δCH_{arom}, opb, 42
134	925	929	964	927	927	0.01	2.62	δCH_{arom}, opb, 41
135	918	917	952	915	915	4.48	0.01	δCH_{arom}, opb, 67
136	918	917	951	915	915	0.01	1.54	δCH_{arom}, opb, 69
137	900	899	943	906	906	0.01	16.43	δCH_{arom}, opb, 54 + νCC, 15 + δNCO, 12
138	900	899	941	904	905	19.48	0.01	δCH_{arom}, opb, 52 + νCC, 16 + δNCO, 13
139	894	899	933	897	897	15.16	0.01	δNCO, 22 + δCH_{arom}, opb, 22 + δCH_{metil}, twist, 12
140	894	899	933	897	897	0.01	6.25	δCH_{arom}, opb, 22 + δNCO, 20 + δCH_{metil}, twist, 12
141	869	870	904	869	869	33.31	0.01	δCCC_{ring}, 81
142	869	870	903	868	868	0.01	7.71	δCCC_{ring}, 80
143	851	853	885	851	851	1.83	0.01	δCH_{arom}, opb, 50 + τCC, 14
144	851	853	885	851	851	0.01	8.99	δCH_{arom}, opb, 52 + τCC, 13
145	829	829	868	835	835	2.49	0.01	δCH_{arom}, opb, 49 + τCC, 10
146	829	829	868	835	835	0.01	5.69	δCH_{arom}, opb, 54
147	829	829	863	830	830	1.64	0.01	δCCC_{ring}, 71
148	829	829	863	830	830	0.01	63.87	δCCC_{ring}, 72
149	815	817	841	808	808	0.01	14.83	δCCC_{ring}, 65 + νCN, 21
150	815	817	840	807	807	3.75	0.01	δCCC_{ring}, 68 + νCN, 22
151	802	795	832	800	800	6.42	0.01	νCC_{arom}, 52 + δCCC_{ring}, 24 + δCNC, 21
152	802	795	832	800	800	0.01	30.57	νCC_{arom}, 54 + δCNC, 24 + δCCC_{ring}, 23
153	779	771	794	763	764	0.01	31.58	γNH, 30 + γC-C_{Carb}, 27
154	779	771	794	763	763	34.18	0.01	γNH, 30 + γC-C_{Carb}, 31
155	741	747	774	744	744	0.01	8.50	δCH_{arom}, opb, 32 + τCC_{ring}, 31 + τCC, 31
156	741	747	773	743	743	33.28	0.01	δCH_{arom}, opb, 31 + τCC_{ring}, 30 + τCC, 27
157	741	747	767	738	738	176.36	0.01	τCC_{ring}, 27 + τCC, 27 + δCH_{arom}, opb, 22

Table 2. Continued.

No	Exp. IR (cm^{-1})	RAMAN (cm^{-1})	B3LYP					Assignments,
			Unscaled (cm^{-1})	Scaled (cm^{-1})	Scaled (cm^{-1})	IR Int. (km/mol)	RAMAN activity (A^4/amu)	PED (%)
158	741	747	766	737	737	0.01	3.42	τCC_{ring}, 35 + τCC, 25 + δCH_{arom}, opb, 23
159	726	724	753	724	724	0.01	7.40	γC_{Carb}, 33 + δCH_{metil}, wagg, 13 + δCH_{arom}, opb, 12
160	719	718	749	720	720	10.10	0.01	γC_{Carb}, 38 + δCH_{arom}, opb, 13 + δCH_{metil}, wagg, 10
161	719	718	744	715	715	48.25	0.01	γNH, 42 + γC-C_{Carb}, 20 + δCH_{arom}, opb, 11
162	719	718	742	713	713	0.01	8.03	γNH, 41 + γC-C_{Carb}, 21 + δCH_{arom}, opb, 14
163	701	705	730	702	702	8.87	0.01	γC_{ring}, 76
164	701	705	730	701	701	0.01	9.23	γC_{ring}, 74
165	697	699	728	700	700	7.69	0.01	γC, 68 + γC_{ring}, 12
166	697	699	727	699	699	0.01	4.05	γC_{ring}, 74
167	691	689	713	685	685	56.42	0.01	νCCl, 61 + δCH_{metil}, wagg, 10
168	691	689	712	684	684	0.01	14.12	νCCl, 62 + δCH_{metil}, wagg, 10
169	678	671	705	678	678	0.01	10.36	νCCl, 60 + δCH_{metil}, wagg, 15
170	678	671	704	677	677	43.90	0.01	νCCl, 64 + δCH_{metil}, wagg, 18
171	649	653	677	651	651	0.01	39.03	γCN, 44
172	649	653	676	650	650	43.40	0.01	γCN, 45
173	638	638	663	637	637	4.33	0.01	δCCC_{ring}, 28 + γC, 21 + δCH_{metil}, wagg, 11
174	638	638	662	636	636	0.01	4.61	δCCC_{ring}, 27 + γC, 20 + δCH_{metil}, wagg, 13
175	614	614	642	618	618	0.01	24.24	δCCC_{ring}, 75 + δNH, opb, 13
176	614	614	642	617	617	15.66	0.01	δCCC_{ring}, 74 + δNH, opb, 14
177	581	592	608	584	584	8.34	0.01	δCCC_{ring}, 44 + δCCN, 20
178	581	592	607	584	584	0.01	16.30	δCCC_{ring}, 43 + δCCN, 20
179	570	582	600	577	577	0.01	24.29	δCCC_{ring}, 53 + δNH, opb, 12
180	570	582	600	576	576	8.48	0.01	δCCC_{ring}, 51 + δNH, opb, 11
181	567	567	577	554	555	79.83	0.01	δCCC_{ring}, 34 + νCCl, 30 + τCC_{ring}, 17
182	567	567	576	553	553	0.01	17.20	δCCC_{ring}, 34 + νCCl, 30 + τCC_{ring}, 17
183	537	540	555	533	533	0.01	2.56	τCC_{ring}, 87
184	537	540	555	533	533	6.45	0.01	τCC_{ring}, 87
185	533	540	552	530	530	12.50	0.01	γC_{ring}, 85
186	533	540	551	530	530	0.01	8.69	γC_{ring}, 84
187	-	484	508	488	488	0.01	3.98	δCCC_{ring}, 61+ γC, 21 + δCH_{metil}, twist, 13
188	-	484	508	488	488	19.32	0.01	δCCC_{ring}, 60 + γC, 22 + δCH_{metil}, twist, 15
189	-	464	475	456	456	0.01	3.13	τCC_{ring}, 63
190	-	464	474	456	456	8.02	0.01	τCC_{ring}, 64
191	-	464	473	455	455	28.29	0.01	τCC_{ring}, 62
192	-	464	473	454	454	0.01	11.91	τCC_{ring}, 82
193	-	442	468	450	450	42.20	0.01	τCC_{ring}, 71
194	-	442	466	448	448	0.01	0.65	γC_{ring}, 53 + δCCN, 20
195	-	425	434	417	417	18.37	0.01	δCCN, 41 + τCC_{ring}, 14
196	-	425	432	416	416	0.01	7.70	δCCN, 45 + τCC_{ring}, 15
197	-	401	417	401	401	131.59	0.01	γNH, 81 + τCC_{ring}, 11
198	-	401	416	400	400	0.01	20.39	γNH, 73 + τCC_{ring}, 12
199	-	391	408	392	392	49.26	0.01	γNH, 33 + νCCl, 29
200	-	391	403	388	388	0.01	15.90	γNH, 33 + νCCl, 12
201	-	372	386	372	372	117.05	0.01	γNH, 28 + δCCC, 21
202	-	372	381	367	367	0.01	14.85	γNH, 75 + δCCC, 13
203	-	320	335	322	322	0.01	2.92	δCCCl, 44 + τCC_{ring}, 30
204	-	320	334	321	321	9.14	0.01	δCCCl 44 + τCC_{ring}, 32
205	-	320	332	319	319	0.01	2.07	δCCC, 23 + τCC_{ring}, 21
206	-	320	331	318	318	6.66	0.01	δCNH, 30 + + τCC_{ring} 18
207	-	314	315	303	303	0.01	10.65	τCC_{ring}, 80
208	-	314	313	300	301	5.72	0.01	τCC_{ring}, 54 + δCCC, 10
209	-	298	308	296	296	5.68	0.01	τCC_{ring}, 63 + δCCC, 12
210	-	298	306	294	294	0.01	4.32	τCC_{ring}, 51 + δCCC, 11
211	-	298	303	292	292	0.01	6.78	τCC_{ring}, 40 + δCCCl, 22 + δCH_{metil}, rock, 15
212	-	298	302	290	290	12.04	0.01	δCCN, 30 + τCC_{ring}, 31 + δCH_{metil}, rock, 14
213	-	260	274	263	263	3.00	0.01	τCC, 25 + + δCCC, 25 + δCCN, 21
214	-	260	273	263	263	0.01	0.85	δCCC, 29 + τCC, 26 + δCCN, 21
215	-	251	265	255	255	18.16	0.01	τCC, 56 + δCH_{metil}, rock, 35
216	-	251	263	253	253	0.01	2.52	τCC, 68 + δCH_{metil}, rock, 31
217	-	238	247	237	237	6.71	0.01	τCC, 58 + δCH_{metil}, rock, 27
218	-	238	245	235	236	0.01	2.35	τCC, 28 + δCH_{metil}, rock, 20
219	-	227	235	226	226	0.01	2.14	τCC, 60 + τCH_{metil}, 21
220	-	227	235	226	226	7.18	0.01	τCC, 65 + τCH_{metil}, 24
221	-	220	227	218	218	20.89	0.01	τCH_{metil}, 24 + τCC, 21 + τCN, 12
222	-	216	225	216	216	0.01	6.57	τCH_{metil}, 21 + τCC, 21 + τCN, 11
223	-	186	199	192	192	7.89	0.01	τCC, 29 + τCH_{metil}, 14 + τNH, 13
224	-	186	198	190	190	0.01	5.24	τCC, 22 + τCH_{metil}, 15 + τNH, 12
225	-	179	182	175	175	0.01	1.68	τCC, 31 + τCN, 21
226	-	169	177	170	170	10.46	0.01	δCCN, 23 + τCC, 21 + τCN, 14
227	-	162	170	164	164	10.15	0.01	τCC, 22 + τCC_{ring}, 20 + δCCO, 16
228	-	162	170	164	164	0.01	4.09	τCC_{ring}, 26 + τCC, 20 + δCCO 19
229	-	155	165	158	158	7.58	0.01	τCC_{ring}, 52 + τCN, 21
230	-	155	163	157	157	0.01	2.66	τCC_{ring}, 51 + τCN, 31
231	-	131	130	125	125	0.01	6.99	τCC_{ring}, 31 + τCC, 30 + δCNC, 10
232	-	-	129	124	124	1.95	0.01	τCC_{ring}, 31 + τCC, 29 + δCNC, 20
233	-	-	107	103	103	0.01	17.58	τNC_{ring}, 23 + νO...H, 18 + τCC_{ring}, 17
234	-	-	107	103	103	9.78	0.01	τNC_{ring}, 28 + τCC_{ring}, 20
235	-	-	98	94	94	0.01	4.99	τNH...OC, 21 + δCCN, 20
236	-	-	94	90	90	9.55	0.01	τNC_{ring}, 38 + τCC, 29

Table 2. Continued.

No	Exp. IR (cm^{-1})	RAMAN (cm^{-1})	B3LYP					Assignments, PED (%)
			Unscaled (cm^{-1})	Scaled (cm^{-1})	Scaled (cm^{-1})	IR Int. (km/mol)	RAMAN activity (A^4/amu)	
237	-	-	81	78	78	3.08	0.01	δCOH, 34 + τNC_{ring}, 22 + τCC_{ring}, 12
238	-	-	79	76	76	0.01	7.22	τNC_{ring}, 38 + τCC, 29
239	-	-	72	69	69	0.01	7.34	τNC_{ring}, 27 + τCN, 21 + τCC, 18
240	-	-	70	67	67	6.83	0.01	δCCN, 32 + τNC_{ring}, 25 + τCC_{ring}, 13
241	-	-	58	56	56	0.01	2.38	τNC_{ring}, 25 + τCC, 15 + τCC_{ring}, 13
242	-	-	54	52	52	2.41	0.01	τCN, 34 + τCC_{ring}, 27 + τNC_{ring}, 26
243	-	-	49	47	47	2.94	0.01	τNC_{ring}, 23 + τCC, 21 + τCN, 10
244	-	-	48	46	46	0.01	4.36	τCN, 26 + τCC_{ring}, 22
245	-	-	42	41	41	1.19	0.01	τCC, 35 + τCN, 28
246	-	-	42	41	41	0.01	2.71	τCC, 36 + τCN, 21
247	-	-	40	39	39	0.01	0.55	τCC, 43
248	-	-	38	37	37	4.34	0.01	τCN, 31 + τCC, 22
249	-	-	37	36	36	0.01	7.48	τCC, 30 + τCN, 11
250	-	-	36	34	34	2.51	0.01	τCC, 40
251	-	-	32	31	31	0.01	2.52	τCC, 21 + τCN, 10
252	-	-	31	30	30	0.89	0.01	τCC, 38
253	-	-	29	28	28	0.01	3.29	τCC, 20 + τCN, 12 + τCO, 10
254	-	-	27	26	26	0.01	4.00	τCC, 26 + τCN, 19
255	-	-	25	24	24	0.38	0.01	τCC_{ring}, 63 + τCC, 16
256	-	-	16	16	16	0.98	0.01	τCC, 19 + δCOH, 15 + τCO...HN, 10
257	-	-	14	13	13	0.01	2.49	τCC, 25 + τNC_{ring}, 10
258	-	-	10	10	10	0.23	0.01	τCN, 16 + τCC, 13
r			0.9999	0.9999	0.9999			
Mean absolute percentage error			3.9085	0.4836	0.4828			
Mean absolute error			59.4301	6.7498	6.7434			
RMS			59.4835	8.9128	8.9123			
Scaling factor			1.0000	0.9614	0.9615			

* ν, stretching; δ, in-plane bending; γ, out-of-plane bending; τ, torsion; ipb: in-plane bending; opb: out-of-plane bending; scis: scissoring; wagg: wagging; twist: twisting; rock: rocking; umbr: umbrella; sym, symmetric; asym, asymmetric; arom: aromatic; carb: carbonyl group; br: Between ring; SF: Scaling factor; CSF: Calculated scaling factor; PED less than 10% are not shown.

Table 3. Statistical comparison of theoretical and experimental vibrational wavenumbers of L^{NNN} molecule on the used method and basis set *.

Method	**B3LYP**	**B3LYP×SF**	**B3LYP×CSF**	**B3LYP**	**B3LYP×SF**	**B3LYP×CSF**
Basis set	**6-31G(d,p)**			**6-311G(d,p)**		
r	0.9999	0.9999	0.9999	0.9999	0.9999	0.9999
Mean absolute percentage error	3.9085	0.4836	0.4828	3.6402	0.7304	0.7250
Mean absolute error	59.4301	6.7498	6.7434	51.8010	8.1959	8.1867
RMS	59.4835	8.9128	8.9123	50.1132	9.0561	9.0357
Scaling factor	1.0000	0.9614	0.9615	1.0000	0.9679	0.9675
Method	**B3PW91**	**B3PW91×SF**	**B3PW91×CSF**	**B3PW91**	**B3PW91×SF**	**B3PW91×CSF**
Basis set	**6-31G(d,p)**			**6-311G(d,p)**		
r	0.9999	0.9999	0.9999	0.9999	0.9999	0.9999
Mean absolute percentage error	4.3650	0.7509	0.7303	3.9508	0.7579	0.7670
Mean absolute error	63.9214	9.1326	8.7367	56.3114	8.8874	8.8026
RMS	62.6507	10.4008	9.8223	54.5543	10.1032	9.7999
Scaling factor	1.0000	0.9573	0.9595	1.0000	0.9631	0.9647
Method	**B-LYP**	**B-LYP×SF**	**B-LYP×CSF**	**B-LYP**	**B-LYP×SF**	**B-LYP×CSF**
Basis set	**6-31G(d,p)**			**6-311G(d,p)**		
r	0.9999	0.9999	0.9999	0.9999	0.9999	0.9999
Mean absolute percentage error	0.8773	0.7574	0.7832	0.7355	0.8774	0.7446
Mean absolute error	13.7557	10.9979	10.7545	10.5338	11.2224	9.9809
RMS	16.7634	12.6458	12.1863	12.3226	12.6502	11.4966
Scaling factor	1.0000	0.9945	0.9922	1.0000	0.9934	0.9970
Method	**mPW1PW**	**mPW1PW×SF**	**mPW1PW×CSF**	**mPW1PW**	**mPW1PW×SF**	**mPW1PW×CSF**
Basis set	**6-31G(d,p)**			**6-311G(d,p)**		
r	0.9999	0.9999	0.9999	0.9999	0.9999	0.9999
Mean absolute percentage error	4.9951	0.6182	0.5865	4.7233	0.8551	0.8722
Mean absolute error	74.9157	8.9412	8.4917	67.0145	9.9435	9.7613
RMS	74.0626	11.2626	10.6256	64.3573	11.1262	10.7601
Scaling factor	1.0000	0.9500	0.9524	1.0000	0.9567	0.9585
Method	**HF**	**HF×SF**	**HF×CSF**	**HF**	**HF×SF**	**HF×CSF**
Basis set	**6-31G(d,p)**			**6-311G(d,p)**		
r	0.9994	0.9994	0.9994	0.9993	0.9993	0.9993
Mean absolute percentage error	11.9216	1.8079	1.9171	11.2904	1.9162	2.0199
Mean absolute error	170.3659	27.0687	27.5107	160.3598	28.0124	28.4236
RMS	161.4518	29.2392	28.8031	151.8008	29.7798	29.4472
Scaling factor	1.0000	0.8992	0.9023	1.0000	0.9051	0.9078

* SF: Scaling factor, CSF: Calculated scaling factor in this research.

3.3. Thermodynamic parameters and molecular properties

The thermodynamic parameters namely energy, zero-point vibrational energy, rotational constants and entropy of the compounds have also been computed at the HF and DFT level using 6-31G(d,p) 6-311G(d,p) basis sets at 298.15 K in ground state. The results of the statistical thermos-chemical analysis of title compound are presented in Table 4. The thermodynamic data provides helpful information for further studies of the title compound. The standard thermodynamic functions can be used as reference thermodynamic values to calculate the changes of entropies and the changes of enthalpies of the reaction.

Table 4. The calculated thermodynamic parameters of L^{NNN} molecule.

Thermodynamic parameters	B3LYP		B3PW91		BLYP		mPW1PW91		HF	
(298 K)	6-31	6-311	6-31	6-311	6-31	6-311	6-31	6-311	6-31	6-311
SCF energy (a.u.)	-3865.093	-3865.668	-3864.117	-3864.652	-3864.220	-3864.839	-3864.660	-3865.193	-3849.643	-3850.131
Total energy (Thermal) E_{total} (kcal/mol)	468.778	466.929	470.147	468.100	455.715	453.766	472.870	470.936	498.299	495.644
Entropy, S (cal/mol.K)	303.739	299.180	298.494	299.637	304.474	308.323	302.180	298.549	297.962	300.663
Vibrational_enegry, E_{vib} (kcal/mol)	467.000	465.151	468.370	466.323	453.938	451.988	471.093	469.159	496.521	493.867
Zero-point vib. energy, E_o (kcal/mol)	437.1447	435.5989	438.9418	436.8083	423.5659	421.4053	441.5041	439.8499	468.2872	465.5137
Rotational constant (GHz)										
A	0.07223	0.07642	0.07725	0.07756	0.07512	0.07356	0.07340	0.07858	0.07187	0.07192
B	0.03983	0.03437	0.03435	0.03448	0.03362	0.03381	0.04031	0.03475	0.03945	0.03916
C	0.03251	0.03081	0.03083	0.03096	0.03007	0.03006	0.03291	0.03128	0.03284	0.03279
Dipole moment (Debye)										
μ_x	0.0000	-0.0003	0.0003	0.0001	0.0002	0.0000	0.0000	-0.0005	0.0000	-0.0006
μ_y	-0.0001	-0.0002	-0.0003	0.0000	0.0000	-0.0003	0.0000	-0.0003	0.0001	-0.0004
μ_z	-0.0001	0.0005	0.0001	0.0001	-0.0002	-0.0001	0.0000	0.0000	0.0002	0.0003
μ_{Total}	0.0001	0.0006	0.0004	0.0002	0.0002	0.0003	0.0000	0.0006	0.0002	0.0008
Entropy (cal/mol.K)										
Total	303.739	299.180	298.494	299.637	304.474	308.323	302.180	298.549	297.962	300.663
Translational	45.756	45.756	45.756	45.756	45.756	45.756	45.756	45.756	45.756	45.756
Rotational	39.372	39.515	39.505	39.492	39.578	39.594	39.332	39.461	39.376	39.384
Vibrational	218.611	213.908	213.233	214.389	219.139	222.973	217.092	213.332	212.829	215.523

* 6-31: 6-31G(d,p); 6-311: 6-311G(d,p).

Atomic charges play an important role in quantum chemistry. The atomic natural charges have been calculated by natural bond orbital (NBO) method [57,58] for the title compound and the results are shown in Table 5. The charge distribution of the title molecule has an important influence on the vibrational spectra. The charges at the site of the C21 atom attached to the O22 atom are more positive than other carbon atoms due to the presence of the electron withdrawing nature of the oxygen atom (O22). Similar trends were observed for the other carbonyl groups. Mulliken atomic charge [59] populations give one of the simplest pictures of charge distribution and the Mulliken charges predict net atomic charges in the molecule (Table 6). Comparing the NBO and the Mulliken charges for the title compound, we can easily say that there is a general agreement for all atoms.

3.4. Hirshfeld surface analysis

In this study, the Hirshfeld surface analyses revealing the nature of intermolecular interactions of the L^{NNN} compound and the two-dimensional (2D) fingerprint plots associated with these surfaces were calculated using the Crystal Explorer17 program [50]. The X-ray single crystal analysis revealed two independent molecules in the asymmetric unit of L^{NNN} (Mol A and Mol B). For this reason, Hirshfeld surface analyzes were performed for both molecules in the asymmetric unit and thus the structure similarities and differences between the independent molecules in the asymmetric unit were shown. Hirshfeld surfaces visualize intermolecular contacts by red-blue-white color-coding for short or long contacts and investigates the properties of all contacts within the crystal lattice.

Hirshfeld surfaces of the molecules A and B mapped with different properties, i.e. d_{norm}, curvedness and shape index and were shown to be transparent to allow visualization of the molecular component in a similar orientation for all of the structures, around which they were calculated (Figure 4). d_{norm} surfaces were used to determine the normalized contact distance of the atoms, defined in terms of the d_i, d_e and van der Waals (vdW) radii. The d_{norm} value is positive or negative when intermolecular interactions are longer or shorter than vdW radii, respectively. The d_{norm} values are mapped on the Hirshfeld surface by using white-blue-red color scales. The white regions seen on the surface are equal to the sum of vdW radii, while the red and blue regions represent interactions at shorter and longer distances than vdW radii, respectively [60].

The shape index and curvedness surfaces are used to determine the characteristic packaging modes, planar stacking arrangements, and the manner in which neighboring molecules contact each other [61]. On the other hand, two-dimensional fingerprint maps were used to quantitatively determine intermolecular interactions in the compound.

When the d_{norm} surfaces of molecules A and B are examined, a total of three red spots appear, which result from the interactions between A and B molecules in the asymmetric unit (Figure 4). The two large red spots on the surfaces are due to strong N–H···O hydrogen bonds between the A and B molecules, while the smaller red spot is caused by the weaker C-H···O interaction (Figure 5). These interactions continue between the ABABABAB molecules along the crystal lattice, causing the molecules to expand along the crystallographic axis (Figure 6).

On the d_{norm} surface of the Mol A, two light red spots are also seen due to C-H···Cl interactions. The C-H···Cl interactions occur between the aromatic ring hydrogen atoms and the chlorine atoms of the 2-chloropropionyl moiety of adjacent the molecules A. These interactions are weaker than the N–H···O and C–H···O interactions (Figure 7).

The C-H···π interactions contributing to the crystal clustering and three-dimensional structure of the synthesized L^{NNN} compound were visualized by means of the Hirshfeld surface mapped by the shape index function. As shown in Figure 8, on the Hirshfeld surface mapped by the shape index function, the hollow orange (π···H) and swollen blue regions (H···π) correspond to C–H···π interactions (Figure 8).

The 2D fingerprint plots associated with Hirshfeld surface analyzes of molecules A and B providing quantitative information for the intermolecular specific atom-to-atom contacts in the crystal lattice. The fingerprint plots were decomposed to highlight particular atom pairs in close contacts. Figure 9 shows the decomposed fingerprint plots of A and B molecules that are crystallographically independent. In the molecules A and B, the H···H (vdW) interactions have the highest contributions of the total Hirshfeld surface with 60.9 and 59.6%, respectively, and the contribution from the H···H contact is 1.3% more for molecule A compared to molecule B.

Table 5. The natural charges of the atoms of L^{NNN} molecule determined by natural bond analysis *.

Atom	Charge									
	B3LYP		B3PW91		BLYP		mPW1PW91		HF	
	6-31	6-311	6-31	6-311	6-31	6-311	6-31	6-311	6-31	6-311
C1	-0.7037	-0.5888	-0.7298	-0.6024	-0.7007	-0.5961	-0.7299	-0.6012	-0.6561	-0.5096
C2	-0.2870	-0.2132	-0.3123	-0.2320	-0.2802	-0.2127	-0.3139	-0.2328	-0.2685	-0.1722
Cl3	-0.0978	-0.0940	-0.0762	-0.0812	-0.1010	-0.1015	-0.0810	-0.0794	-0.1063	-0.1163
C4	0.6812	0.6792	0.6765	0.6744	0.6372	0.6412	0.6877	0.6829	0.8372	0.8259
O5	-0.6024	-0.6080	-0.6011	-0.6042	-0.5739	-0.5825	-0.6053	-0.6091	-0.7005	-0.6906
N6	-0.6526	-0.6297	-0.6478	-0.6293	-0.6161	-0.6048	-0.6623	-0.6358	-0.7485	-0.7215
C7	0.1276	0.1374	0.1276	0.1339	0.1257	0.1328	0.1254	0.1356	0.1313	0.1414
C8	-0.2350	-0.2036	-0.2465	-0.2092	-0.2379	-0.2047	-0.2432	-0.2095	-0.1999	-0.1592
C9	-0.2470	-0.1996	-0.2494	-0.2043	-0.2383	-0.2010	-0.2567	-0.2035	-0.2527	-0.2037
C10	-0.2355	-0.1989	-0.2481	-0.2041	-0.2380	-0.1993	-0.2443	-0.2046	-0.2117	-0.1642
C11	-0.2712	-0.2192	-0.2622	-0.2249	-0.2507	-0.2213	-0.2819	-0.2241	-0.2733	-0.2297
C12	0.1412	0.1439	0.1273	0.1401	0.1241	0.1395	0.1402	0.1403	0.1861	0.1935
N13	-0.6368	-0.6619	-0.6757	-0.6613	-0.6485	-0.6381	-0.6442	-0.6656	-0.7177	-0.6953
C14	0.1570	0.1625	0.1418	0.1589	0.1371	0.1540	0.1557	0.1620	0.2057	0.2172
C15	-0.2797	-0.2353	-0.2758	-0.2418	-0.2626	-0.2310	-0.2903	-0.2446	-0.2876	-0.2473
C16	-0.2210	-0.1923	-0.2430	-0.1980	-0.2313	-0.1922	-0.2297	-0.1986	-0.2003	-0.1508
C17	-0.2570	-0.2023	-0.2513	-0.2079	-0.2389	-0.2020	-0.2666	-0.2097	-0.2616	-0.2156
C18	-0.2219	-0.2084	-0.2500	-0.2148	-0.2389	-0.2069	-0.2301	-0.2160	-0.1988	-0.1589
C19	0.1055	0.1276	0.1172	0.1233	0.1159	0.1249	0.1028	0.1231	0.1176	0.1287
N20	-0.6319	-0.5967	-0.6159	-0.5960	-0.5876	-0.5766	-0.6397	-0.6008	-0.7226	-0.6934
C21	0.7091	0.7012	0.7015	0.6964	0.6594	0.6609	0.7160	0.7063	0.8664	0.8557
O22	-0.6870	-0.7143	-0.6993	-0.7120	-0.6667	-0.6827	-0.6928	-0.7194	-0.7847	-0.7821
C23	-0.2958	-0.2174	-0.3197	-0.2361	-0.2883	-0.2155	-0.3213	-0.2374	-0.2789	-0.1787
C24	-0.6999	-0.5839	-0.7264	-0.5968	-0.6989	-0.5915	-0.7250	-0.5954	-0.6559	-0.5033
Cl25	-0.0855	-0.0859	-0.0664	-0.0732	-0.0907	-0.0946	-0.0697	-0.0718	-0.0972	-0.1097
C26	-0.7037	-0.5888	-0.7298	-0.6024	-0.7007	-0.5961	-0.7299	-0.6012	-0.6561	-0.5096
C27	-0.2870	-0.2132	-0.3123	-0.2320	-0.2802	-0.2127	-0.3139	-0.2328	-0.2685	-0.1722
Cl28	-0.0978	-0.0940	-0.0762	-0.0812	-0.1010	-0.1015	-0.0810	-0.0794	-0.1063	-0.1163
C29	0.6812	0.6792	0.6765	0.6744	0.6372	0.6412	0.6877	0.6829	0.8372	0.8259
O30	-0.6024	-0.6080	-0.6011	-0.6042	-0.5739	-0.5825	-0.6053	-0.6091	-0.7005	-0.6906
N31	-0.6526	-0.6297	-0.6478	-0.6293	-0.6161	-0.6048	-0.6623	-0.6357	-0.7485	-0.7215
C32	0.1276	0.1374	0.1276	0.1339	0.1257	0.1328	0.1254	0.1356	0.1313	0.1414
C33	-0.2350	-0.2036	-0.2465	-0.2092	-0.2379	-0.2047	-0.2432	-0.2095	-0.1999	-0.1592
C34	-0.2470	-0.1996	-0.2494	-0.2043	-0.2383	-0.2010	-0.2567	-0.2035	-0.2527	-0.2037
C35	-0.2355	-0.1989	-0.2481	-0.2041	-0.2380	-0.1993	-0.2443	-0.2046	-0.2117	-0.1642
C36	-0.2712	-0.2191	-0.2622	-0.2249	-0.2507	-0.2213	-0.2819	-0.2241	-0.2733	-0.2296
C37	0.1412	0.1439	0.1273	0.1401	0.1241	0.1395	0.1402	0.1403	0.1861	0.1935
N38	-0.6368	-0.6619	-0.6757	-0.6613	-0.6485	-0.6381	-0.6442	-0.6656	-0.7177	-0.6953
C39	0.1570	0.1625	0.1418	0.1589	0.1371	0.1540	0.1557	0.1619	0.2057	0.2172
C40	-0.2797	-0.2353	-0.2758	-0.2418	-0.2626	-0.2310	-0.2903	-0.2446	-0.2876	-0.2473
C41	-0.2210	-0.1923	-0.2430	-0.1980	-0.2313	-0.1922	-0.2297	-0.1986	-0.2003	-0.1508
C42	-0.2570	-0.2023	-0.2513	-0.2079	-0.2389	-0.2020	-0.2666	-0.2097	-0.2616	-0.2156
C43	-0.2219	-0.2084	-0.2500	-0.2148	-0.2389	-0.2069	-0.2301	-0.2160	-0.1988	-0.1589
C44	0.1055	0.1276	0.1172	0.1233	0.1159	0.1249	0.1028	0.1231	0.1176	0.1287
N45	-0.6319	-0.5967	-0.6159	-0.5960	-0.5876	-0.5766	-0.6397	-0.6008	-0.7226	-0.6933
C46	0.7091	0.7012	0.7015	0.6964	0.6594	0.6609	0.7160	0.7063	0.8664	0.8557
O47	-0.6870	-0.7143	-0.6993	-0.7120	-0.6667	-0.6826	-0.6928	-0.7194	-0.7847	-0.7821
C48	-0.2958	-0.2174	-0.3197	-0.2361	-0.2883	-0.2155	-0.3213	-0.2374	-0.2789	-0.1787
C49	-0.6999	-0.5839	-0.7264	-0.5968	-0.6989	-0.5915	-0.7250	-0.5954	-0.6559	-0.5033
Cl50	-0.0855	-0.0859	-0.0664	-0.0732	-0.0907	-0.0946	-0.0697	-0.0718	-0.0972	-0.1097
H51	0.2531	0.2087	0.2572	0.2135	0.2476	0.2119	0.2629	0.2128	0.2395	0.1880
H52	0.2446	0.2075	0.2577	0.2124	0.2482	0.2103	0.2534	0.2121	0.2281	0.1778
H53	0.2644	0.2247	0.2742	0.2297	0.2631	0.2262	0.2733	0.2294	0.2511	0.1997
H54	0.2735	0.2136	0.2782	0.2192	0.2668	0.2146	0.2834	0.2192	0.2668	0.1951
H55	0.4448	0.4194	0.4500	0.4233	0.4373	0.4141	0.4516	0.4252	0.4529	0.4171
H56	0.2715	0.2388	0.2815	0.2444	0.2706	0.2389	0.2801	0.2446	0.2557	0.2112
H57	0.2432	0.2042	0.2523	0.2091	0.2414	0.2046	0.2524	0.2093	0.2361	0.1899
H58	0.2418	0.2033	0.2509	0.2082	0.2399	0.2036	0.2510	0.2085	0.2342	0.1874
H59	0.2479	0.2111	0.2562	0.2174	0.2443	0.2113	0.2577	0.2178	0.2412	0.1978
H60	0.4362	0.4030	0.4427	0.4093	0.4306	0.4015	0.4445	0.4092	0.4408	0.3970
H61	0.2561	0.2224	0.2670	0.2290	0.2548	0.2216	0.2660	0.2299	0.2489	0.2066
H62	0.2461	0.2073	0.2558	0.2123	0.2446	0.2073	0.2553	0.2128	0.2376	0.1901
H63	0.2454	0.2076	0.2560	0.2125	0.2449	0.2075	0.2547	0.2132	0.2376	0.1919
H64	0.2529	0.2265	0.2701	0.2330	0.2584	0.2243	0.2615	0.2340	0.2460	0.2013
H65	0.4437	0.4235	0.4568	0.4273	0.4431	0.4175	0.4516	0.4287	0.4524	0.4136
H66	0.2924	0.2304	0.3027	0.2387	0.2873	0.2286	0.3040	0.2404	0.2828	0.2067
H67	0.2506	0.2056	0.2566	0.2107	0.2458	0.2079	0.2595	0.2105	0.2357	0.1825
H68	0.2571	0.2145	0.2657	0.2189	0.2561	0.2171	0.2661	0.2184	0.2441	0.1904
H69	0.2618	0.2291	0.2733	0.2334	0.2647	0.2325	0.2705	0.2326	0.2465	0.1953
H70	0.2531	0.2087	0.2572	0.2135	0.2476	0.2119	0.2629	0.2128	0.2395	0.1880
H71	0.2446	0.2075	0.2577	0.2124	0.2482	0.2103	0.2534	0.2121	0.2281	0.1778
H72	0.2644	0.2247	0.2742	0.2297	0.2631	0.2262	0.2733	0.2294	0.2511	0.1997
H73	0.2735	0.2136	0.2782	0.2192	0.2668	0.2146	0.2834	0.2192	0.2668	0.1951
H74	0.4448	0.4194	0.4500	0.4233	0.4373	0.4141	0.4516	0.4252	0.4529	0.4171
H75	0.2715	0.2388	0.2815	0.2444	0.2706	0.2389	0.2801	0.2446	0.2557	0.2112
H76	0.2432	0.2042	0.2523	0.2091	0.2414	0.2046	0.2524	0.2093	0.2361	0.1899
H77	0.2418	0.2033	0.2509	0.2082	0.2399	0.2036	0.2510	0.2085	0.2342	0.1874
H78	0.2479	0.2111	0.2562	0.2174	0.2443	0.2113	0.2577	0.2178	0.2412	0.1978

Table 5. Continued.

Atom	Charge									
	B3LYP		B3LYP		B3LYP		B3LYP		B3LYP	B3LYP
	6-31	6-31	6-31	6-31	6-31	6-31	6-31	6-31	6-31	6-31
H79	0.4362	0.4030	0.4427	0.4093	0.4306	0.4015	0.4445	0.4092	0.4408	0.3970
H80	0.2561	0.2224	0.2670	0.2290	0.2548	0.2216	0.2660	0.2299	0.2489	0.2066
H81	0.2461	0.2073	0.2558	0.2123	0.2446	0.2073	0.2553	0.2128	0.2376	0.1901
H82	0.2454	0.2076	0.2560	0.2125	0.2449	0.2075	0.2547	0.2132	0.2376	0.1919
H83	0.2529	0.2265	0.2701	0.2330	0.2584	0.2243	0.2615	0.2340	0.2460	0.2013
H84	0.4437	0.4235	0.4568	0.4273	0.4431	0.4175	0.4516	0.4287	0.4524	0.4136
H85	0.2924	0.2304	0.3027	0.2387	0.2873	0.2286	0.3040	0.2404	0.2828	0.2067
H86	0.2571	0.2145	0.2657	0.2189	0.2561	0.2171	0.2661	0.2184	0.2441	0.1904
H87	0.2506	0.2056	0.2566	0.2107	0.2458	0.2078	0.2595	0.2105	0.2357	0.1825
H88	0.2618	0.2291	0.2733	0.2334	0.2647	0.2325	0.2705	0.2327	0.2465	0.1953

* 6-31: 6-31G(d,p); 6-311: 6-311G(d,p).

Table 6. Mulliken charges of the atoms of L^{NNN} molecule *.

Atom	Charge									
	B3LYP		B3PW91		BLYP		mPW1PW91		HF	
	6-31	6-311	6-31	6-311	6-31	6-311	6-31	6-311	6-31	6-311
C1	-0.2922	-0.2331	-0.3661	-0.2715	-0.2597	-0.2238	-0.3694	-0.2713	-0.3072	-0.1589
C2	-0.2844	-0.3820	-0.3494	-0.4424	-0.2508	-0.3667	-0.3599	-0.4467	-0.3205	-0.3625
Cl3	-0.0937	-0.1034	-0.0631	-0.0835	-0.1000	-0.1121	-0.0670	-0.0804	-0.0976	-0.1391
C4	0.6159	0.4233	0.6356	0.4499	0.5766	0.3813	0.6412	0.4586	0.7812	0.5969
O5	-0.4919	-0.3549	-0.4936	-0.3637	-0.4655	-0.3208	-0.4980	-0.3692	-0.5830	-0.4675
N6	-0.6653	-0.4782	-0.6947	-0.5170	-0.6024	-0.4327	-0.7095	-0.5268	-0.8377	-0.6314
C7	0.2705	0.1828	0.2843	0.2000	0.2789	0.1666	0.2689	0.2061	0.2478	0.1826
C8	-0.0882	-0.0630	-0.1211	-0.0673	-0.0794	-0.0620	-0.1164	-0.0625	-0.1004	-0.0293
C9	-0.1055	-0.0999	-0.1412	-0.1116	-0.0751	-0.0927	-0.1503	-0.1096	-0.1746	-0.1089
C10	-0.0925	-0.0862	-0.1293	-0.0947	-0.0648	-0.0794	-0.1350	-0.0921	-0.1431	-0.0721
C11	-0.1222	-0.0704	-0.1311	-0.0776	-0.0827	-0.0674	-0.1576	-0.0728	-0.1670	-0.1135
C12	0.2871	0.0857	0.2288	0.0802	0.2429	0.0930	0.2847	0.0710	0.2990	0.2086
N13	-0.7373	-0.5310	-0.7369	-0.5663	-0.6764	-0.4891	-0.7731	-0.5727	-0.8569	-0.6674
C14	0.3071	0.1251	0.2387	0.1227	0.2522	0.1184	0.3005	0.1248	0.3118	0.2627
C15	-0.1317	-0.0967	-0.1483	-0.1056	-0.0971	-0.0863	-0.1668	-0.1026	-0.1834	-0.1375
C16	-0.0878	-0.0857	-0.1320	-0.0961	-0.0677	-0.0753	-0.1289	-0.0972	-0.1374	-0.0612
C17	-0.1131	-0.1015	-0.1388	-0.1160	-0.0701	-0.0939	-0.1580	-0.1145	-0.1809	-0.1271
C18	-0.0762	-0.0588	-0.1184	-0.0621	-0.0784	-0.0556	-0.0992	-0.0603	-0.1095	-0.0462
C19	0.2245	0.1354	0.2609	0.1434	0.2595	0.1253	0.2136	0.1437	0.2218	0.1511
N20	-0.6166	-0.4318	-0.6547	-0.4675	-0.5582	-0.3891	-0.6597	-0.4753	-0.7895	-0.5899
C21	0.6319	0.4380	0.6501	0.4637	0.5729	0.3926	0.6633	0.4752	0.8042	0.5869
O22	-0.5484	-0.4521	-0.5623	-0.4637	-0.5150	-0.4082	-0.5617	-0.4729	-0.6631	-0.5577
C23	-0.2719	-0.3142	-0.3355	-0.3666	-0.2377	-0.3059	-0.3487	-0.3697	-0.3065	-0.2691
C24	-0.3100	-0.2551	-0.3855	-0.2953	-0.2843	-0.2431	-0.3861	-0.2952	-0.3349	-0.2000
Cl25	-0.0793	-0.1065	-0.0516	-0.0901	-0.0884	-0.1126	-0.0529	-0.0890	-0.0833	-0.1380
C26	-0.2922	-0.2331	-0.3661	-0.2715	-0.2597	-0.2238	-0.3694	-0.2713	-0.3072	-0.1589
C27	-0.2844	-0.3819	-0.3494	-0.4424	-0.2508	-0.3667	-0.3599	-0.4467	-0.3205	-0.3625
Cl28	-0.0937	-0.1034	-0.0631	-0.0835	-0.1000	-0.1121	-0.0670	-0.0804	-0.0976	-0.1391
C29	0.6159	0.4233	0.6356	0.4499	0.5766	0.3813	0.6412	0.4586	0.7812	0.5969
O30	-0.4919	-0.3549	-0.4936	-0.3637	-0.4655	-0.3208	-0.4980	-0.3692	-0.5830	-0.4675
N31	-0.6653	-0.4782	-0.6947	-0.5170	-0.6024	-0.4327	-0.7095	-0.5268	-0.8377	-0.6314
C32	0.2705	0.1828	0.2843	0.2000	0.2789	0.1666	0.2689	0.2061	0.2478	0.1827
C33	-0.0882	-0.0630	-0.1211	-0.0673	-0.0795	-0.0620	-0.1164	-0.0625	-0.1004	-0.0293
C34	-0.1055	-0.0999	-0.1412	-0.1116	-0.0751	-0.0927	-0.1503	-0.1096	-0.1746	-0.1089
C35	-0.0925	-0.0862	-0.1293	-0.0947	-0.0648	-0.0794	-0.1350	-0.0921	-0.1431	-0.0721
C36	-0.1222	-0.0703	-0.1311	-0.0776	-0.0827	-0.0674	-0.1576	-0.0728	-0.1670	-0.1134
C37	0.2871	0.0855	0.2288	0.0802	0.2428	0.0930	0.2847	0.0710	0.2990	0.2086
N38	-0.7373	-0.5309	-0.7369	-0.5663	-0.6764	-0.4891	-0.7731	-0.5727	-0.8569	-0.6674
C39	0.3071	0.1250	0.2387	0.1227	0.2522	0.1184	0.3005	0.1248	0.3118	0.2626
C40	-0.1317	-0.0967	-0.1483	-0.1056	-0.0971	-0.0863	-0.1668	-0.1026	-0.1834	-0.1375
C41	-0.0878	-0.0857	-0.1320	-0.0961	-0.0677	-0.0753	-0.1289	-0.0972	-0.1374	-0.0612
C42	-0.1131	-0.1015	-0.1388	-0.1160	-0.0701	-0.0939	-0.1580	-0.1145	-0.1809	-0.1270
C43	-0.0762	-0.0588	-0.1184	-0.0621	-0.0784	-0.0556	-0.0992	-0.0603	-0.1095	-0.0462
C44	0.2245	0.1355	0.2609	0.1434	0.2595	0.1253	0.2136	0.1437	0.2218	0.1511
N45	-0.6166	-0.4318	-0.6547	-0.4675	-0.5582	-0.3891	-0.6597	-0.4753	-0.7895	-0.5899
C46	0.6319	0.4380	0.6501	0.4637	0.5729	0.3926	0.6633	0.4753	0.8042	0.5869
O47	-0.5484	-0.4521	-0.5623	-0.4637	-0.5150	-0.4082	-0.5617	-0.4729	-0.6631	-0.5577
C48	-0.2719	-0.3142	-0.3355	-0.3666	-0.2377	-0.3059	-0.3487	-0.3697	-0.3065	-0.2691
C49	-0.3100	-0.2551	-0.3855	-0.2953	-0.2843	-0.2431	-0.3861	-0.2952	-0.3349	-0.2000
Cl50	-0.0793	-0.1065	-0.0516	-0.0901	-0.0884	-0.1126	-0.0529	-0.0890	-0.0833	-0.1379
H51	0.1275	0.1167	0.1468	0.1332	0.1081	0.1122	0.1575	0.1332	0.1418	0.1077
H52	0.1127	0.1253	0.1452	0.1406	0.1049	0.1202	0.1415	0.1409	0.1251	0.1056
H53	0.1530	0.1491	0.1808	0.1656	0.1418	0.1422	0.1802	0.1660	0.1640	0.1333
H54	0.1778	0.2140	0.2031	0.2368	0.1553	0.2062	0.2103	0.2381	0.2119	0.2038
H55	0.3014	0.2593	0.3114	0.2698	0.2662	0.2445	0.3260	0.2736	0.3591	0.2928
H56	0.1291	0.1335	0.1698	0.1477	0.1042	0.1221	0.1703	0.1457	0.1887	0.1207
H57	0.0883	0.0969	0.1263	0.1069	0.0624	0.0879	0.1306	0.1056	0.1542	0.0995
H58	0.0862	0.0949	0.1237	0.1051	0.0594	0.0857	0.1286	0.1038	0.1533	0.0993
H59	0.0987	0.1007	0.1313	0.1155	0.0643	0.0918	0.1429	0.1134	0.1666	0.1136
H60	0.2722	0.2357	0.3011	0.2493	0.2599	0.2251	0.2977	0.2495	0.3304	0.2566
H61	0.1103	0.1213	0.1483	0.1371	0.0821	0.1104	0.1540	0.1365	0.1772	0.1278
H62	0.0951	0.1031	0.1331	0.1129	0.0689	0.0939	0.1374	0.1116	0.1604	0.1050

Table 6. Continued.

Atom	Charge									
	B3LYP		B3LYP		B3LYP		B3LYP		B3LYP	
	6-31	6-31	6-31	6-31	6-31	6-31	6-31	6-31	6-31	6-31
H63	0.0934	0.0979	0.1322	0.1072	0.0680	0.0892	0.1355	0.1055	0.1582	0.1053
H64	0.1154	0.1449	0.1550	0.1636	0.0891	0.1313	0.1545	0.1629	0.1844	0.1351
H65	0.2901	0.2650	0.3192	0.2749	0.2727	0.2507	0.3161	0.2770	0.3494	0.2833
H66	0.1928	0.2297	0.2233	0.2572	0.1714	0.2148	0.2314	0.2631	0.2236	0.2172
H67	0.1373	0.1286	0.1582	0.1448	0.1190	0.1231	0.1650	0.1456	0.1469	0.1177
H68	0.1381	0.1403	0.1636	0.1551	0.1243	0.1352	0.1674	0.1550	0.1541	0.1288
H69	0.1517	0.1574	0.1826	0.1755	0.1486	0.1530	0.1790	0.1746	0.1612	0.1353
H70	0.1275	0.1167	0.1468	0.1332	0.1081	0.1121	0.1575	0.1332	0.1418	0.1077
H71	0.1127	0.1253	0.1452	0.1406	0.1049	0.1202	0.1415	0.1409	0.1251	0.1056
H72	0.1530	0.1491	0.1808	0.1656	0.1418	0.1422	0.1802	0.1660	0.1640	0.1333
H73	0.1778	0.2140	0.2031	0.2368	0.1553	0.2062	0.2103	0.2381	0.2119	0.2038
H74	0.3014	0.2593	0.3114	0.2698	0.2662	0.2445	0.3260	0.2736	0.3591	0.2928
H75	0.1291	0.1335	0.1698	0.1477	0.1042	0.1221	0.1703	0.1457	0.1887	0.1207
H76	0.0883	0.0969	0.1263	0.1069	0.0624	0.0879	0.1306	0.1056	0.1542	0.0995
H77	0.0862	0.0949	0.1237	0.1051	0.0594	0.0857	0.1286	0.1038	0.1533	0.0993
H78	0.0987	0.1007	0.1313	0.1155	0.0643	0.0918	0.1429	0.1134	0.1666	0.1136
H79	0.2722	0.2356	0.3011	0.2493	0.2599	0.2251	0.2977	0.2495	0.3304	0.2566
H80	0.1103	0.1213	0.1483	0.1371	0.0821	0.1104	0.1540	0.1365	0.1772	0.1278
H81	0.0951	0.1031	0.1331	0.1129	0.0689	0.0939	0.1374	0.1116	0.1604	0.1050
H82	0.0934	0.0979	0.1322	0.1072	0.0680	0.0892	0.1355	0.1055	0.1582	0.1053
H83	0.1154	0.1449	0.1550	0.1636	0.0891	0.1313	0.1545	0.1629	0.1844	0.1351
H84	0.2901	0.2650	0.3192	0.2749	0.2727	0.2507	0.3161	0.2770	0.3494	0.2833
H85	0.1928	0.2297	0.2233	0.2572	0.1714	0.2148	0.2314	0.2631	0.2236	0.2172
H86	0.1381	0.1403	0.1636	0.1551	0.1243	0.1352	0.1674	0.1550	0.1541	0.1288
H87	0.1373	0.1286	0.1582	0.1448	0.1190	0.1231	0.1650	0.1456	0.1469	0.1177
H88	0.1517	0.1574	0.1826	0.1755	0.1486	0.1530	0.1790	0.1746	0.1612	0.1354

* 6-31: 6-31G(d,p); 6-311: 6-311G(d,p).

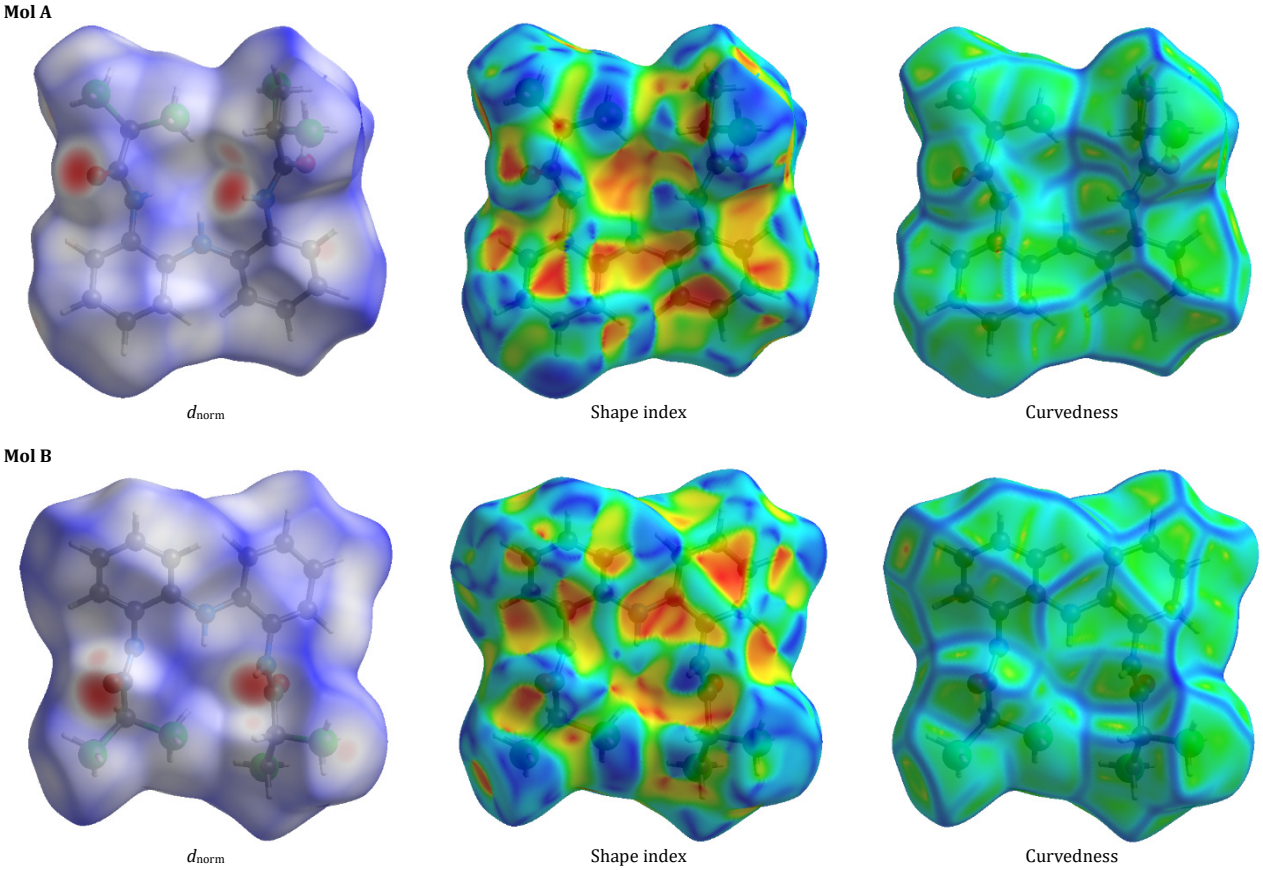

Figure 4. Hirshfeld surfaces mapped with d_{norm}, shape index and curvedness for L^{NNN} (Mol A and Mol B).

Despite the high share of H···H interactions, the role of these interactions in the stabilization of the crystal structure is quite small in importance because H···H interactions are between the same species. The C···H contacts, which refer to the C-H···π interactions described previously, contribute 21.3 (for Mol A) and 23.6% (for Mol B) of the Hirshfeld surfaces with $d_i + d_e \approx 2.8$ Å. On the other hands, although the contribution of H···O/O···H interactions to the Hirshfeld surface is 14.7% and 13.8%, respectively, these interactions are the strongest interactions with $d_i + d_e \approx 1.9$ Å, and their roles in stabilizing the crystal structure is quite large.

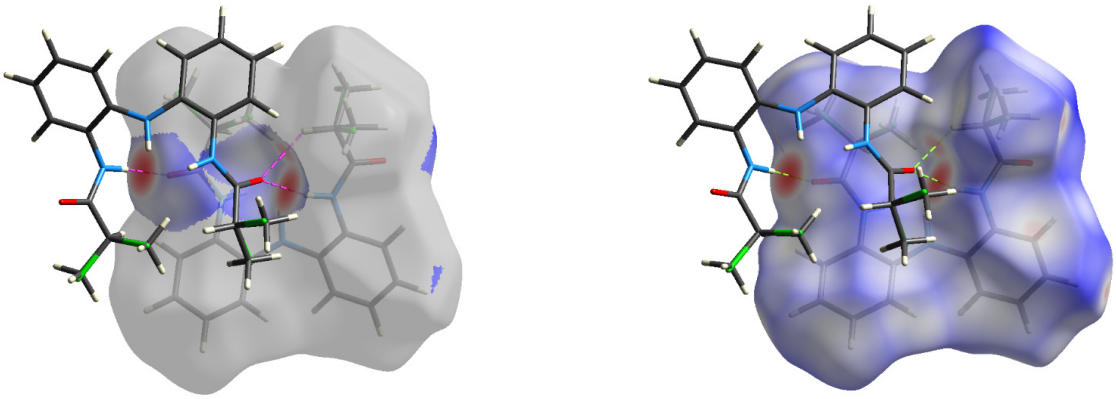

Figure 5. N–H···O and C-H···O interactions between A and B molecules on Hirshfeld surface mapped by d_{norm} function.

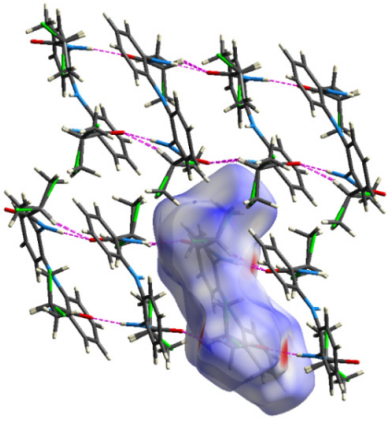

Figure 6. Consequtive N–H···O and C-H···O interactions between the A and B molecules in the crystal lattice along the crystallographic [010] axis.

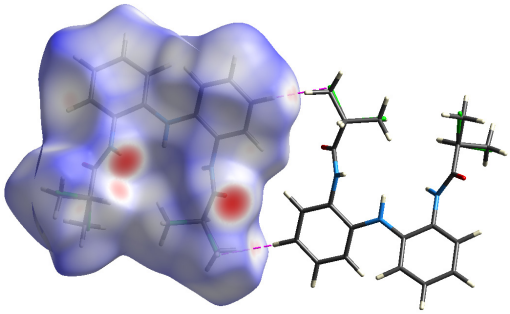

Figure 7. C-H···Cl interactions between molecules A on Hirshfeld surface mapped by d_{norm} function.

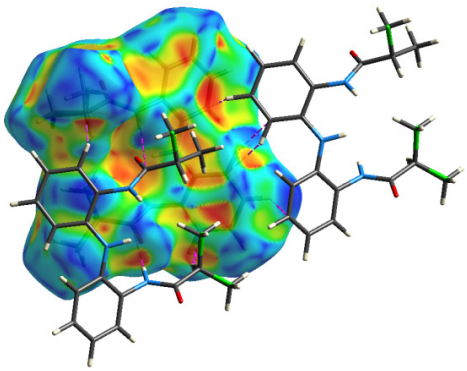

Figure 8. C–H···π interactions between two adjacent molecules on the Hirshfeld surface mapped by the shape index function.

Mol A

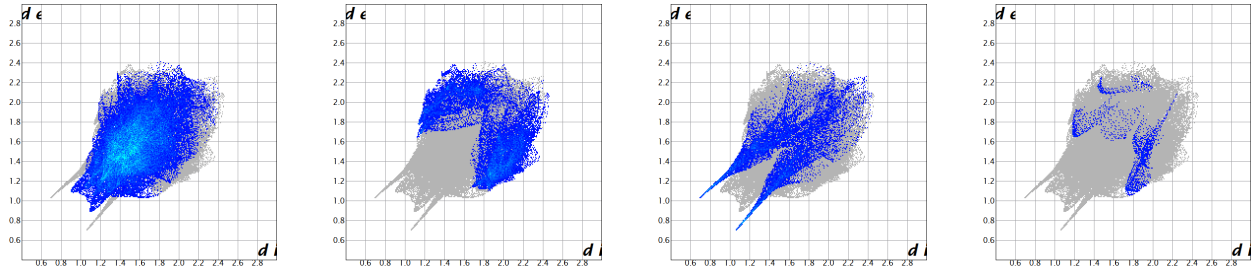

H···H 60.9% C···H/H···C 21.3% O···H/H···O 14.7% N···H/H···N 2.1%

Mol B

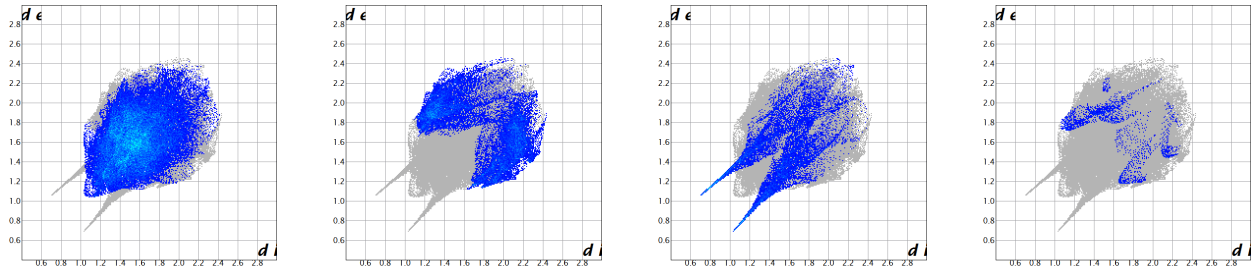

H···H 59.6% C···H/H···C 23.6% O···H/H···O 13.8% N···H/H···N 2.2%

Figure 9. Decomposed 2D fingerprint plots of A and B molecules.

4. Conclusion

The present investigation thoroughly analyzed both the vibrational spectra, infrared and RAMAN of the title compound. All the vibrational bands observed in the IR and RAMAN spectra of the investigated compound are assigned to various modes of vibration. The complete vibrational assignments of wavenumbers are made on the basis of potential energy distribution. The second aim of this work was to discover which method yields the most accurate results simultaneously for the IR and RAMAN frequencies as well as for the geometrical parameters of the title compound. The scaled B3LYP/6-31G(d,p) results are the best among the used methods. Thermodynamic properties such as energy, entropy, and enthalpy are also calculated. The presented structural and spectroscopic data of the title compound in this research can be used in the future in the analysis of similar compounds. In addition, the present quantum chemical study may lead to the understanding of properties and reactivity of redox active compounds. On the other hand, the 3D Hirshfeld surface analysis and 2D fingerprint plots revealed that the O···H/H···O interactions represent an important contribution of the Hirshfeld surface result of hydrogen-bonding interactions in the molecules A and B.

Acknowledgements

This study was supported by Research Fund of Mersin University in Turkey with Project Number: 2018-1-TP2-2800.

Supporting information

CCDC-1954366 contains the supplementary crystallographic data for this paper. These data can be obtained free of charge via https://www.ccdc.cam.ac.uk/structures/, or by e-mailing data request@ccdc.cam.ac.uk, or by contacting The Cambridge Crystallographic Data Centre, 12 Union Road, Cambridge CB2 1EZ, UK; fax: +44(0)1223-336033.

Disclosure statement

Conflict of interests: The authors declare that they have no conflict of interest.
Author contributions: All authors contributed equally to this work.
Ethical approval: All ethical guidelines have been adhered.
Sample availability: Samples of the compounds are available from the author.

Funding

Mersin University
http://dx.doi.org/10.13039/501100004172

ORCID

Aysegul Suzan Polat
http://orcid.org/0000-0002-0281-4011
Ilkay Gumus
http://orcid.org/0000-0002-9398-0057
Hakan Arslan
http://orcid.org/0000-0003-0046-9442

References

[1]. Lyaskovskyy, V.; Bruin, B. *Am. Chem. Soc. Catal.* **2012**, *2*, 270-279.
[2]. Allgeier, A. M.; Mirkin, C. A. *Angew. Chem., Int. Edit.* **1998** *37*, 894-908.
[3]. Wile, B. M.; Trovitch, R. J.; Bart, S. C.; Tondreau, A. M.; Lobkovsky, E.; Milsmann, C.; Bill, E.; Wieghardt, K.; Chirik, P. J. *Inorg. Chem.* **2009**, *48(9)*, 4190-4200.
[4]. Bart, S. C.; Lobkovsky, E.; Bill, E.; Chirik; P. J. *J. Am. Chem. Soc.* **2006**, *128(16)*, 5302-5303.
[5]. Tondreau, A. M.; Milsmann, C.; Patrick, A. D.; Hoyt, H. M.; Lobkovsky, E.; Wieghardt, K.; Chirik, P. J. *J. Am. Chem. Soc.* **2010**, *132(42)*, 15046-15059.
[6]. Skabara, P. J.; Pozo-Gonzalo, C.; Lardies, M. N.; Laguna, M.; Cerrada, E.; Luquin, A.; Gonzalez, B.; Coles, S. J.; Hursthouse, M. B.; Harrington, R. W.; Clegg, W. *Dalton Trans.* **2008**, *23*, 3070-3079.
[7]. Mukherjee, C.; Pieper, U.; Bothe, E.; Bachler, V.; Bill, E.; Weyhermuller, T.; Chaudhuri, *P. Inorg. Chem.* **2008**, *47(19)*, 8943-8956.
[8]. Zhu, D.; Thapa, I.; Korobkov, I.; Gambarotta, S.; Budzelaar, *P. H. M. Inorg. Chem.* **2011**, *50*, 9879-9887.

[9]. Dzik, W. I.; Van Der Vlugt, J. I.; Reek, J. N. H.; De Bruin, B. *Angew. Chem., Int. Ed.* **2011**, *50*, 3356-3358.
[10]. Hindson, K.; De Bruin, B. *Eur. J. Inorg. Chem.* **2012**, *3*, 340-580.
[11]. Kaim, W. *Coord. Chem. Rev.* **1987**, *76*, 187-235.
[12]. Chirik, P.J. *Inorg. Chem.* **2011**, *50(20)*, 9737-9914.
[13]. Van der Vlugt, J. I., *Eur. J. Inorg. Chem.* **2012**, *3*, 363-375.
[14]. Dzik, W. I.; Zhang, P. X.; de Bruin, B. *Inorg. Chem.* **2011**, *50(20)*, 9896-9903.
[15]. Kaim, W. *Coord. Chem. Rev.* **2010**, *254*, 1580-1588.
[16]. Nawn, G.; Waldie, K. M.; Oakley, S. R.; Peters, B. D.; Mandel, D.; Patrick, B. P.; McDonald, R.; Hicks, R. G. *Inorg. Chem.* **2011**, *50*, 9826-9837.
[17]. Bowman, A. C.; Milsmann, C.; Hojilla, A. C. C.; Lobkovsky, E.; Wieghardt, K.; Chirik, P. J. *J. Am. Chem. Soc.* **2010**, *132(5)*, 1676-1684.
[18]. Bowman, C. A.; Milsmann, C.; Bill, E.; Lobkovsky, E.; Weyhermüller, T.; Wieghardt, K.; Chirik, P. J. *Inorg. Chem.* **2010**, *49(13)*, 6110-6123.
[19]. Manuel, T. D.; Rohde, J. U. *Am. Chem. Soc.* **2009**, *131(43)*, 15582-15583.
[20]. Rolle, C. J.; Hardcastle, K. I.; Soper, J. D. *Inorg. Chem.* **2008**, *47(6)*, 1892-1894.
[21]. Vlcek, A. *Coord. Chem. Rev.* **2010**, *254(13-14)*, 1357-1357.
[22]. Ward, M. D.; McCleverty, J. A. *J. Chem. Soc. Dalton Trans.* **2002**, *3*, 275-288.
[23]. Smith, A. L.; Hardcastle, K. I.; Soper, J. D. *J. Am. Chem. Soc.* **2010**, *132*, 14358-14360.
[24]. Arslan, H. Ligand design studies for metal catalyzed oxidation reactions, TUBITAK Project no: 112T322, 2012.
[25]. Polat, A. S., MSc Thesis, Mersin University, Mersin, Turkey, 2019.
[26]. Polat, A. S.; Gumus, I.; Arslan, H. Int. Eng. Nat. Sci. Conf. Book, Diyarbakir, Turkey, 2019.
[27]. Aydogdu, S. I., MSc Thesis, Mersin University, Mersin, Turkey, 2019.
[28]. Aydogdu, I.; Gumus, I.; Arslan, H. Int. Eng. Nat. Sci. Conf. Book, Diyarbakir, Turkey, 2019.
[29]. Frisch, M. J.; Trucks, G. W.; Schlegel, H. B.; Scuseria, G. E.; Robb, M. A.; Cheeseman, J. R.; Scalmani, G.; Barone, V.; Petersson, G. A.; Nakatsuji, H.; Li, X.; Caricato, M.; Marenich, A. V.; Bloino, J.; Janesko, B. G.; Gomperts, R.; Mennucci, B.; Hratchian, H. P.; Ortiz, J. V.; Izmaylov, A. F.; Sonnenberg, J. L.; Williams-Young, D.; Ding, F.; Lipparini, F.; Egidi, F.; Goings, J.; Peng, B.; Petrone, A.; Henderson, T.; Ranasinghe, D.; Zakrzewski, V. G.; Gao, J.; Rega, N.; Zheng, G.; Liang, W.; Hada, M.; Ehara, M.; Toyota, K.; Fukuda, R.; Hasegawa, J.; Ishida, M.; Nakajima, T.; Honda, Y.; Kitao, O.; Nakai, H.; Vreven, T.; Throssell, K.; Montgomery, J. A.; Jr.; Peralta, J. E.; Ogliaro, F.; Bearpark, M. J.; Heyd, J. J.; Brothers, E. N.; Kudin, K. N.; Staroverov, V. N.; Keith, T. A.; Kobayashi, R.; Normand, J.; Raghavachari, K.; Rendell, A. P.; Burant, J. C.; Iyengar, S. S.; Tomasi, J.; Cossi, M.; Millam, J. M.; Klene, M.; Adamo, C.; Cammi, R.; Ochterski, J. W.; Martin, R. L.; Morokuma, K.; Farkas, O.; Foresman, J. B.; Fox, D. J. Gaussian 16, Revision C.01, Gaussian, Inc.; Wallingford CT, 2016.
[30]. Dennington, R.; Keith, T. A.; Millam, J. M. GaussView, Version 6, Semichem Inc.; Shawnee Mission, KS, 2016.
[31]. Moller, C.; Plesset, M.S. *Phys. Rev.* **1934**, *46(7)*, 618-622.
[32]. Becke, A.D. *J. Chem. Phys.* **1993**, *98(7)*, 5648-5652.
[33]. Lee, C.; Yang, W.; Parr, R.G. *Phys. Rev. B* **1988**, *37(2)*, 785-789.
[34]. Adamo, C.; Barone, V. *J. Chem. Phys.* **1998**, *108(2)*, 664-675.
[35]. Burke, K.; Perdew, J.P.; Wang, Y.; Dobson, J.F.; Vignale, G. M.P. Das (Eds.), Electronic Density Functional Theory: Recent Progress and New Directions, Plenum Press, New York, 1998.
[36]. Predew, J.P.; Wang, Y. *Phys. Rev. B* **1992**, *45(23)*, 13244-13249.
[37]. Foresman, B.; Frisch, E. Exploring Chemistry with Electronic Structure Methods: a Guide to Using Gaussian, Gaussian Pitttsburg, PA, 1993.
[38]. Scott, A. P.; Radom, L. *J. Chem.* **1996**, *100*, 16502-16513.
[39]. Arslan, H.; Algul, O.; Dundar, Y. *Vib. Spectrosc.* **2007**, *44*, 248-255
[40]. Arslan, H.; Algul, O. *Spectrochim. Acta A* **2008**, *70*, 109-116
[41]. Yabalak, E.; Gunay, F.; Kasumov, V.; Arslan, H. *Spectrochim. Acta A* **2013**, *110*, 291-303
[42]. Arslan, H.; Mansuroglu, D.; Vanderveer, D.; Binzet, G. *Spectrochim. Acta A* **2009**, *72*, 561-571.
[43]. Arslan, H.; Demircan, A. *Int. J. Mol. Sci.* **2007**, *8*, 1064-1082.
[44]. Arslan, H.; Floerke, U.; Kulcu, N.; Binzet, G. *Spectrochim. Acta A* **2007**, *68*, 1347-1355.
[45]. Panchenko, Y. N. *J. Mol. Struct.* **2001**, *567-568*, 217-230.
[46]. Rauhut, G.; Pulay, P. *J. Phys. Chem.* **1995**, *99(10)*, 3093-3100.
[47]. Arslan, H. Performance Analysis of Vibrational Frequencies, 1.0, Mersin, Turkey, 2007.
[48]. Reed, A. E.; Curtiss, L. A.; Weinhold, F. *Chem. Rev.* **1988**, *88(6)*, 899-926.
[49]. Glendening, E. D.; Reed, A. E.; Carpenter, J. E.; Weinhold, F. *J. Am. Chem. Soc.* **1998**, *120(46)*, 12051-12068.
[50]. Turner, M. J.; McKinnon, J. J.; Wolff, S. K.; Grimwood, D. J.; Spackman, P. R.; Jayatilaka, D.; Spackman, M. A. CrystalExplorer17, University of Western Australia, http://hirshfeldsurface.net, 2017.
[51]. Socrates, G. Infrared and Raman Characteristic Group Frequencies, John Wiley & Sons Ltd. Chichester, 2001.
[52]. Silverstein, R.M.; Webster, F.X.; Kiemle, D.J.; Bryce, D.J. Spectrometric Identification of Organic Compounds, Wiley, 2014.
[53]. Colt, N. B.; Daly, L. H.; Wiberly S. E. Introduction to Infrared and Raman Spectroscopy, 3th edition, Academic Press, Boston, 1990.
[54]. Lebas, J. M.; Garrigou-Lagrange, C.; Josien, M. L. *Spectrochim. Acta* **1959**, *15*, 225-235.
[55]. Wiberley, S. E.; Bunce, S. C.; Bauner, W. H. *Anal. Chem.* **1960**, *32*, 217-221.
[56]. Linvien, D.; Cothup, N.B.; Fateley, W.G.; Graselli, J.G., The Handbook of Infrared and Raman Characteristic Frequencies of Organic Molecules, Academic Press, Boston, 1991.
[57]. Beaula, T. J.; Joe, I. H.; Rastogi, V. K.; Jothy, V. B. *Chem. Phys. Lett.* **2015**, *624*, 93-101.
[58]. Abraham, C. S.; Prasana, J. C.; Muthu, S. *Spectrochim. Acta Mol. Biomol Spectrosc.* **2017**, *181*, 153-163.
[59]. Mulliken, R.S. *J. Chem. Phys.* **1955**, *23*, 1833-1840.
[60]. Wang, J. W.; Zhang, Y. W.; Wang, M. X.; Luo, Y. H.; Sun, B. W. *Polyhedron* **2017**, *124*, 243-250.
[61]. Spackman, M. A.; Jayatilaka, D. *Cryst. Eng. Commun.* **2009**, *11*, 19-32.